

Template for Preparation of Manuscripts for *Nano Research*

This template is to be used for preparing manuscripts for submission to *Nano Research*. Use of this template will save time in the review and production processes and will expedite publication. However, use of the template is not a requirement of submission. Do not modify the template in any way (delete spaces, modify font size/line height, etc.). If you need more detailed information about the preparation and submission of a manuscript to *Nano Research*, please see the latest version of the Instructions for Authors at <http://www.thenanoresearch.com/>.

TABLE OF CONTENTS (TOC)

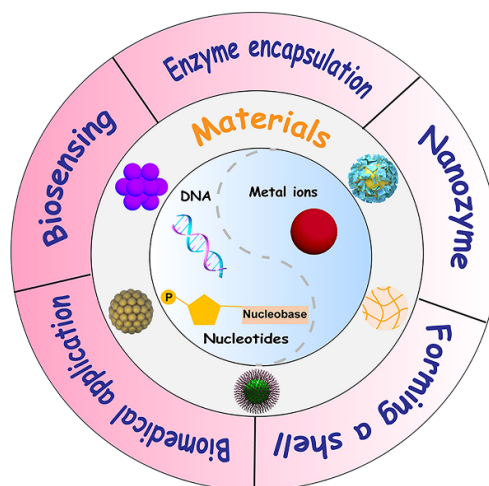
Authors are required to submit a graphic entry for the Table of Contents (TOC) in conjunction with the manuscript title. This graphic should capture the readers' attention and give readers a visual impression of the essence of the paper. Labels, formulae, or numbers within the graphic must be legible at publication size. Tables or spectra are not acceptable. Color graphics are highly encouraged. The resolution of the figure should be at least 600 dpi. The size should be at least 50 mm × 80 mm with a rectangular shape (ideally, the ratio of height to width should be less than 1 and larger than 5/8). One to two sentences should be written below the figure to summarize the paper. To create the TOC, please insert your image in the template box below. Fonts, size, and spaces should not be changed.

Nucleobase, nucleoside, nucleotide and oligonucleotide coordinated metal ions for sensing and biomedicine applications

Jiaojiao Zhou^{1,2}, Heyou Han^{1,*}, and Juewen Liu^{2,*}

1 State Key Laboratory of Agricultural Microbiology, College of Food Science and Technology, Huazhong Agricultural University, Wuhan 430070, China

2 Department of Chemistry, Waterloo Institute for Nanotechnology, University of Waterloo, Waterloo, Ontario N2L 3G1, Canada



This review describes the strategies for the synthesis of nanoparticles, nanofibers and hydrogels through coordination assembly of nucleotides or DNA and metal ions, and introduces their diverse applications in biosensing, drug delivery, catalysis, enzyme immobilization, and surface modification.

Provide the authors' website if possible.

Heyou Han, <http://hyhan.hzau.edu.cn/>

Juewen Liu, <http://www.science.uwaterloo.ca/~liujw/index.html>

Nucleobase, nucleoside, nucleotide and oligonucleotide coordinated metal ions for sensing and biomedicine applications

Jiaojiao Zhou^{1,2}, Heyou Han¹ (✉), and Juewen Liu² (✉)

¹ State Key Laboratory of Agricultural Microbiology, College of Food Science and Technology, Huazhong Agricultural University, Wuhan 430070, China

² Department of Chemistry, Waterloo Institute for Nanotechnology, University of Waterloo, Waterloo, Ontario N2L 3G1, Canada

© Tsinghua University Press and Springer-Verlag GmbH Germany, part of Springer Nature 2020

Received: day month year / **Revised:** day month year / **Accepted:** day month year (automatically inserted by the publisher)

ABSTRACT

Metal ions play critical roles in chemical, biological, and environmental processes. Various biomolecules have the ability to coordinate with metal ions and form various materials. Nucleobases, nucleosides and nucleotides, as the essential components of DNA, have emerged as a useful building block for the construction of functional nanomaterials. In recent years, DNA oligonucleotides have also been used for this purpose. We herein review the strategies for the synthesis of soft and nanomaterials through the assembly of nucleotides or DNA and metal ions to yield various nanoparticles, fibers, and hydrogels. Such coordination methods are simple to operate and can be carried out under ambient conditions. The luminescence, catalytic and molecular recognition properties of these coordination materials are described with representative recent examples. Their applications ranging from biosensing, enzyme encapsulation, catalysis, templated shell growth to cancer therapy are highlighted. Finally, challenges of this field and future perspectives are discussed.

KEYWORDS

Nucleotides, DNA, Metal ions, Self-assembly, Nanostructures

1 Introduction

Metal ions are critical elements in biological systems [1-4]. Some metals such as Na⁺, K⁺, Ca²⁺, Mg²⁺, Zn²⁺, Cu²⁺, and Fe³⁺ are essential, while others especially heavy metal ions (e.g., Hg²⁺ and Pb²⁺), are biologically toxic [5-7]. Regardless of toxicity, many metal ions work in biology through coordination with biomolecules including amino acids, peptides, proteins, nucleobases, and saccharides. For instance, the high affinity between Hg²⁺ and cysteine residues in proteins leads to dysfunction of cells due to the formation of metal-enzyme complexes [8]. While most previous work focused on amino acid and protein based metal coordination, nucleotides and nucleic acids have received growing interest in recent years [9-12]. Some biomolecules can produce nanoscale materials with metal ions, in a way similar to metal-organic frameworks. We call them coordination polymers (CPs) since they are mostly non-crystalline [13-15]. Due to their diverse structures with multiple functional groups, rich metal-binding sites, high biocompatibility, and chirality, they open the possibility of designing functional materials using natural biomolecules instead of synthetic ligands as building blocks.

Nucleotides are interesting ligands for metal ions [11, 16, 17]. Their nucleobases and phosphate groups endow them with excellent metal coordination properties for both soft and hard metals [18]. For example, thymine-thymine mismatches specifically bind to Hg²⁺ to form T-Hg²⁺-T base pairs [19, 20], and cytosine-cytosine mismatches can recognize Ag⁺ to form C-Ag⁺-C pairs [21, 22]. In addition, the difference in the number of phosphate units yield various nucleotides with different structures and metal binding functions [23]. For example, Kimizuka's group studied the self-assembly of

nucleotides with Tb³⁺. ATP significantly amplified the luminescence intensity of Tb³⁺, while AMP and adenosine induced little emission. This was mainly attributed to the coordination by the phosphate groups in the nucleotides [24].

DNA is also a metal ligand [10, 25]. Unlike the simple nucleotides, DNA possesses unique properties with numerous sequences, programmable assembly, and specific molecular recognition functions. Similar to nucleotides, DNA interacts with metal ions via its both phosphate backbone and nucleobases [11].

There is now much research into nucleotide-metal coordination complexes and supramolecular assembly [13, 15, 26-28]. Zhou et al. summarized their structures and properties from crystallography and supramolecular chemistry [15]. Tang and coworkers reviewed the concept for the construction of nanoscale biocoordination polymers through replacement of synthetic organic molecules with natural biomolecules as building blocks [27]. The properties and functions of nucleobase, nucleoside, and nucleotide CPs have also been reviewed [14, 26, 29], and nucleotide-lanthanide complexes have been a focus of research.

Herein, we highlight the progress on transition metals. In addition, we extended our discussion to DNA oligonucleotides as ligands. They form nanoparticles, nanoclusters, nanoshells, hydrogels, and fibers, exhibiting excellent luminescence, molecular recognition ability, and enzyme-like activities. In addition, relevant applications in biosensing, enzyme encapsulation, catalysis, drug/gene delivery, and cancer therapy are also reviewed. Finally, some challenges and future perspectives associated with such coordination complexes are

discussed.

2 Metal coordination by nucleotides and DNA oligonucleotides

DNA has four types of nucleobases, including adenine (A), guanine (G), cytosine (C), and thymine (T) (Fig. 1). Nucleosides are composed of a nucleobase and a deoxyribose ring, which become nucleotides when at least one phosphate unit is attached. The important metal binding sites in the nucleobases are highlighted in blue circles (Fig. 1), which include most of the nitrogen and oxygen atoms except for the exocyclic amines. For nucleotides, their phosphate groups tend to bind hard metal ions [30].

Forming large scale coordination nanomaterials is benefited from the multiple metal binding sites and high coordination flexibility of nucleotides. For AMP, the N1 and N7 positions are both coordination sites at pH 4-9. In purine nucleotides, metal ions interact with a phosphate group as well as N7 in the purine residue because N7 is orientated toward the phosphate group [31, 32]. The N3 and the phosphate group in CMP are both potential metal coordination sites. Multiple coordinated modes exist in nucleotides given the different affinities of nucleotide ligands for metal ions, which is important for the self-assembly of nucleotides and metal ions to form large network structures.

Phosphate-binding metal ions such as Mg^{2+} can stabilize DNA double helix by neutralization of the negative charges on the DNA. Base-binding metal ions, however, destabilize duplex DNA by competing with the hydrogen bonds between base pairs [33]. Some metal ions can also induce a B-Z transition in DNA [34]. For instance, the interaction of double-stranded DNA with Mn^{2+} was investigated by Andrushchenko et al. at different metal/DNA molar ratios using vibrational circular dichroism and infrared absorption spectroscopy [35]. A small amount of DNA adopted the Z conformation at metal/DNA molar ratios below 0.6, whereas a complete transition to the Z-form occurred at ratios above 1.7. At a low metal/DNA molar ratio, Mn^{2+} mainly binds to the phosphate groups, while binding with nitrogen bases is predominant at higher ratios, resulting in partial denaturation of the B-form DNA.

Metal ions could also lead to DNA condensation and aggregation [36-38], which is especially notable for polyvalent metal ions [39, 40]. In the presence of Mn^{2+} , DNA aggregation occurred easily in a relatively wide range of experimental conditions, whereas DNA condensation occurred only in specific conditions [41].

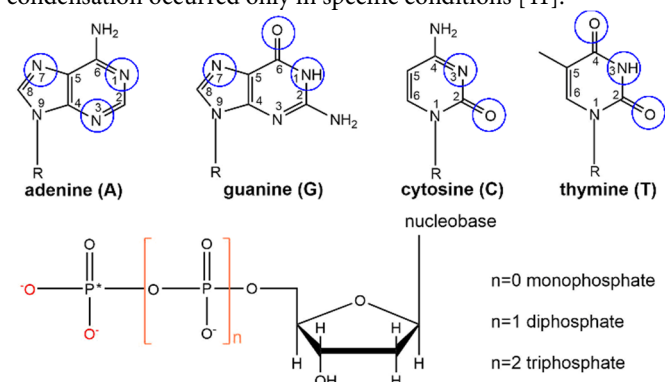


Figure 1 Chemical structures of the nucleobases, nucleosides and nucleotides. The metal coordination sites in the nucleobases are circled.

3 Coordination materials based on metal ions and nucleobases and its derivatives

As discussed above, many interesting materials are formed when metal ions are mixed with nucleobases and derivatives. Herein, we delineate the synthesis of various functional materials based on this type of coordination interactions.

3.1 Formation of nucleotide-based nanomaterials

Nucleobases and their derivatives can self-assemble and form different types of nanomaterials when mixed with metal ions because of their excellent and versatile metal coordination properties.

Subnanometer metal clusters have attracted considerable interest due to their extraordinary optical, biological, and catalytic characteristics. Wu's group prepared fluorescent AMP-capped gold nanoclusters (AuNCs) [42]. The high luminescence was attributed to both the binding of the purine ring and/or the phosphate moiety of AMP as well as their orientations around the gold core. Moreover, electron-rich atoms such as nitrogen and oxygen, or groups such as $-NH_2$ in the ligands can promote the luminescence emission of the AuNCs. Later, this group investigated the influence of pressure on the structure and luminescence properties of AuNCs [43]. It revealed that the orientation of AMP on the gold surface played a crucial role in regulating the luminescence performance.

Utilizing adenosine cyclic monophosphate (cAMP) as templates, tryptophan-stabilized AuNCs (Trp-cAMP-AuNCs) were prepared by a hydrothermal reaction, which exhibited a surprisingly strong luminescence with a quantum yield of 59.6% [44]. The interaction between indole groups and gold atoms plays an important role for the thermal stability of the luminescence. Wang et al. proposed a simple, one-pot synthetic method to prepare nucleoside-templated fluorescent copper nanoclusters [45], which were more cost-effective. Adenosine, cytidine, and guanosine as templates could generate blue emission, but thymidine or the blank (absence of nucleosides) failed. The order of quantum yield of nucleoside-templated copper nanoclusters was $A > C > G \gg T$, which was attributed to the affinity of nucleoside for Cu^{2+} , the electron-donating capability and quenching efficiency of nucleosides. Using CMP and GMP as both stabilizing and reducing agents, Fu et al. synthesized Pt nanoclusters with laccase mimicking activity [46]. Our lab prepared adenosine, AMP and ATP coordinated gold under reducing conditions. Using mass spectrometry, gold-gold interactions were believed to be critical for its emission properties [47].

Nanoparticles are typically between 1 and 100 nm that show size-dependent properties [48]. Pu et al. developed a green synthesis method of silver NPs using nucleotides as templates (Fig. 2) [49]. GMP and $SrCl_2$ formed nanofibers with diameters of 40-90 nm and lengths up to micrometers. Meanwhile, nucleotides including GMP and AMP formed nanoparticles with irregular morphology and different sizes with $EuCl_3$. The nanofibers and nanoparticles were then incubated with $AgNO_3$ under sunlight irradiation. The resulting AgNPs had different colors and localized surface plasmon resonance (LSPR) properties when the GMP/ Sr^{2+} nanofibers, AMP/ $EuCl_3$ and GMP/ $EuCl_3$ nanoparticles were used as templates, and the AgNPs had sizes ranged from 4.8 to 6.1 nm with good monodispersity. Interestingly, when Ag^+ ions were added into the product of

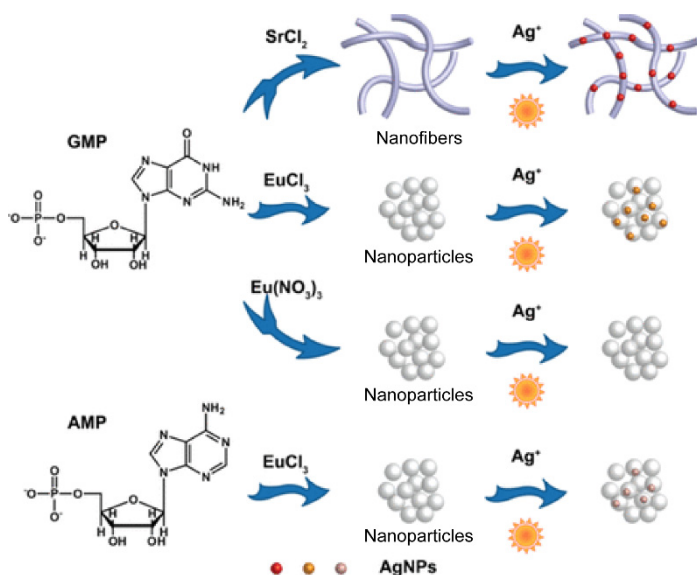


Figure 2 Schematic illustration of the formation of AgNPs mediated by nucleotide-based assemblies and sun light irradiation. Reproduced with permission from ref. [49]. © American Chemical Society 2018.

GMP/Eu(NO₃)₃, no color change was observed after irradiation, implying that the AgNPs could not form in the absence of Cl⁻.

Hybrid nanomaterials containing more than one metal species or ligand were also synthesized. Wu's group synthesized photosensitive gold and silver bimetallic nanoclusters protected by AMP (Au-AgNCs@AMP) [50]. The Au-AgNCs@AMP formed a core-shell structure, where the gold atoms were in the core and the silver atoms were distributed on the surface as a shell. The photosensitivity of the Au-AgNCs@AMP resulted from the hydroxyl groups on the sugar ring of AMP reduced Ag⁺ to Ag(0), which then deposited on the surface of the nanoclusters and further accelerated particle growth. Later, this group also involved polyethylenimine (PEI) and performed a two-stage assembly [51]. PEI assembled with the nanoclusters through electrostatic interactions, which led to a large luminescence enhancement and a blue-shift.

3.2 Formation of hydrogels

Hydrogels are made of crosslinked polymer networks and a large amount of water is trapped inside. Hydrogels exhibit a wide range of applications such as sensing, controlled release, catalysis, and tissue engineering [26]. Nucleobases and their derivatives have also been mixed with metal ions to form hydrogels. For example, Tang et al. described a biocompatible supramolecular hydrogel (C-B-C•Ag⁺) based on the orthogonal formation of cytidine borate diesters with Ag⁺ ions [52]. Both cytidine's ribose and its nucleobase were required to form the hydrogel. The rapid gel-to-sol transitions of C-B-C•Ag⁺ hydrogel induced by shear stress enabled its use for 3D printing of a flexible medical patch.

Sharma et al. reported that thymine and uracil formed spontaneous hydrogels through coordination with Cd²⁺ ions in an alkaline medium [53]. Na₂S was introduced into these systems to generate CdS quantum dots (QDs) within the hydrogels with tunable emission properties from blue to white to yellow. In another work, the authors demonstrated the spontaneous formation of hydrogels and nanoflowers through supramolecular interactions of Zn²⁺ ions and nucleobases [54]. The interaction of cytosine and guanine with Zn²⁺ at alkaline pH resulted in the formation of metallogels with a

nanofibrous morphology (Fig. 3(a)). Furthermore, mixing Zn²⁺ ions with a solution containing a mixture of cytosine and guanine led to the formation of flower-shaped crystalline particles. Both the hydrogels and nanoflowers showed semiconducting properties and were exploited as photocatalysts for the degradation of pollutant organic dyes such as methylene blue and methyl orange.

Adenine derivatives can also coordinate with metal ions to form gels. Our group reported that hydrogels were formed by mixing AMP and lanthanides (Fig. 3(b)) [16]. Non-gel products were obtained upon mixing Dy³⁺ with GMP or CMP, while a gel was produced for Dy³⁺ and AMP. Reacting Dy³⁺ with adenine and its derivatives, only AMP promoted gel formation, whereas clear solutions were observed with the rest. Therefore, both the base structure and the monophosphate are important for gel formation. When Tm³⁺ was mixed with AMP at different ratios by keeping their total concentration at 21 mM, the system was quite tolerant of excess AMP, whereas excess of Tm³⁺ lowered the yield of the gel. We proposed that lanthanides can interact with both the phosphate and the adenine base. TEM characterization showed that AMP/Dy³⁺ and AMP/Lu³⁺ formed fibers consistent with their hydrogel properties.

Recently, Hu et al. reported a supramolecular hydrogel formed by Mn²⁺ and AMP and investigated the factors influencing the mechanical strength and stability of the AMP-Mn hydrogel (Fig. 3(c)) [55]. The gelation process was affected by the concentration of both AMP and Mn²⁺. Increasing the Mn²⁺ concentration from 10 to 50 mM, the turbidity of the hydrogels gradually increased and then remained constant. Similarly, with the increase of the concentration of AMP, the sample changed from sol to a transparent gel and eventually to a turbid gel. However, after storage of the gel for several days at room temperature, a few microspheres appeared, suggesting a low stability of the hydrogel. Increasing the Mn²⁺ concentration as well as temperature would accelerate the formation of the microspheres. In addition, a number of other hydrogels were reported via the assembly of nucleosides, nucleotides, and their derivatives [29, 56, 57].

3.3 Formation of nanofibers

Nanofibers have a large aspect ratio, and they differ from hydrogels by not forming a crosslinked network structure. Nanofibers typically have a diameter of tens of nanometers and length of micrometers [58]. Recently, Qu's group reported Sr²⁺-mediated right-handed helical G-quartet nanofibers, in which GMP was selected as a building block and Sr²⁺ was acted as an initiator and stabilizer [59] (Fig. 4). When K⁺ ions were added to a mixture of GMP and Sr²⁺, left-handed helical G-quartet nanofibers were also obtained, and their diameter and length were similar to those of the GMP/Sr²⁺ nanofibers. The self-assembly of GMP induced the formation of G-quartet structures through hydrogen bonding of the guanine units, which gradually grew into long nanofibers. Dyes such as thioflavin T (ThT), TO, and pyronin Y (PY) co-assembled with these nanofibers can realize full-color right/left circularly polarized luminescence (R-/L-CPL). Efficient energy transfer from ThT to TO and then to PY occurred when the three dyes were intercalated in the nanofibers simultaneously. Such a two-step FRET-CPL indicated a potential application as a nanoscale photoelectric device.

Very Recently, Suo et al. also reported the G-quartet-based nanofiber formation by the self-assembly of GMP with metal ions [64]. Right-handed helical fibers were obtained with Sr²⁺ as an

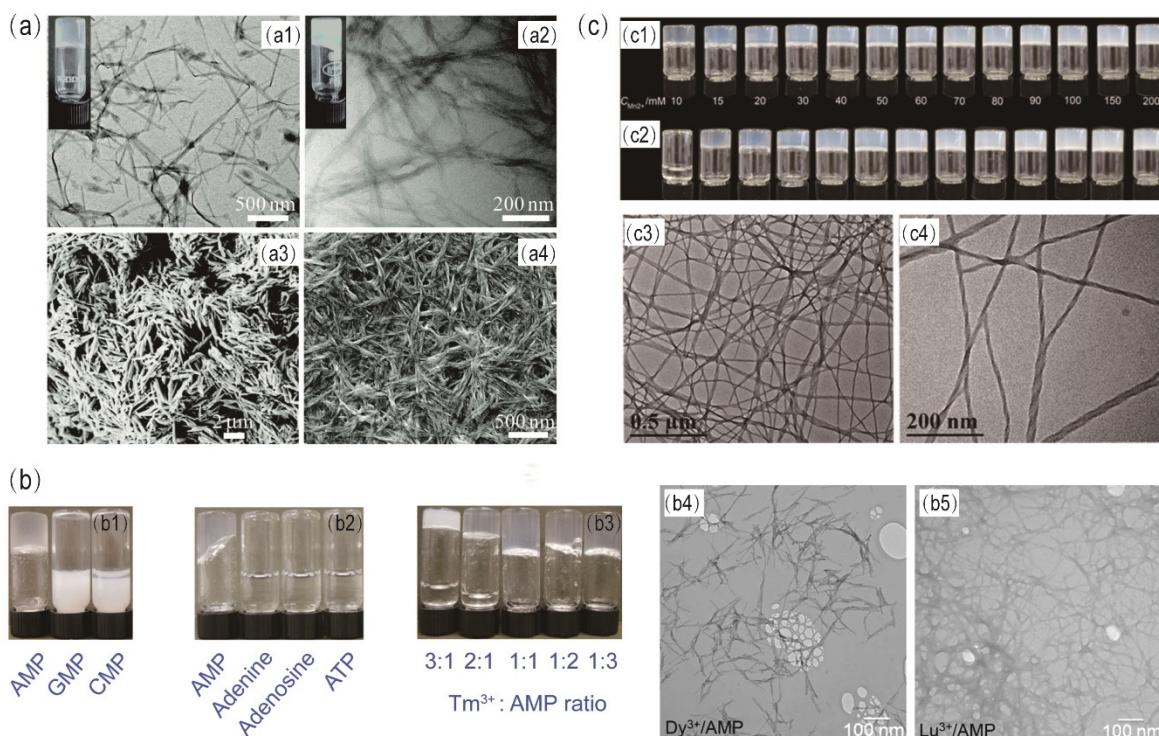


Figure 3 (a) Synthesis of metallogels using cytosine or guanine with Zn^{2+} ions. ((a1) and (a2)) TEM images, ((a3) and (a4)) Field emission scanning electron microscopy images of Zn-cytosine and Zn-guanine hydrogels, respectively; inset: photographs of the two gels. Reproduced with permission from ref. [54]. © Royal Society of Chemistry 2018. (b) Synthesis of hydrogels based on $\text{Ln}^{3+}/\text{AMP}$ coordination. Photographs of the products formed between Dy^{3+} with different (b1) nucleotides or (b2) adenine and its derivatives. (b3) Varying the ratios while keeping the sum of Tm^{3+} and AMP concentrations at 21 mM. TEM micrographs of the CPs formed by mixing AMP with (b4) Dy^{3+} , and (b5) Lu^{3+} . Reproduced with permission from ref. [16]. © American Chemical Society 2018. (c) Synthesis of AMP-Mn hydrogels. Photographs of AMP-Mn hydrogels formed by (c1) 50 mM CMP mixed with 10 to 200 mM Mn^{2+} and (c2) 50 mM Mn^{2+} mixed with 10 to 200 mM AMP. ((c3) and (c4)) TEM images of the AMP-Mn hydrogel. Reproduced with permission from ref. [55]. © American Chemical Society 2020.

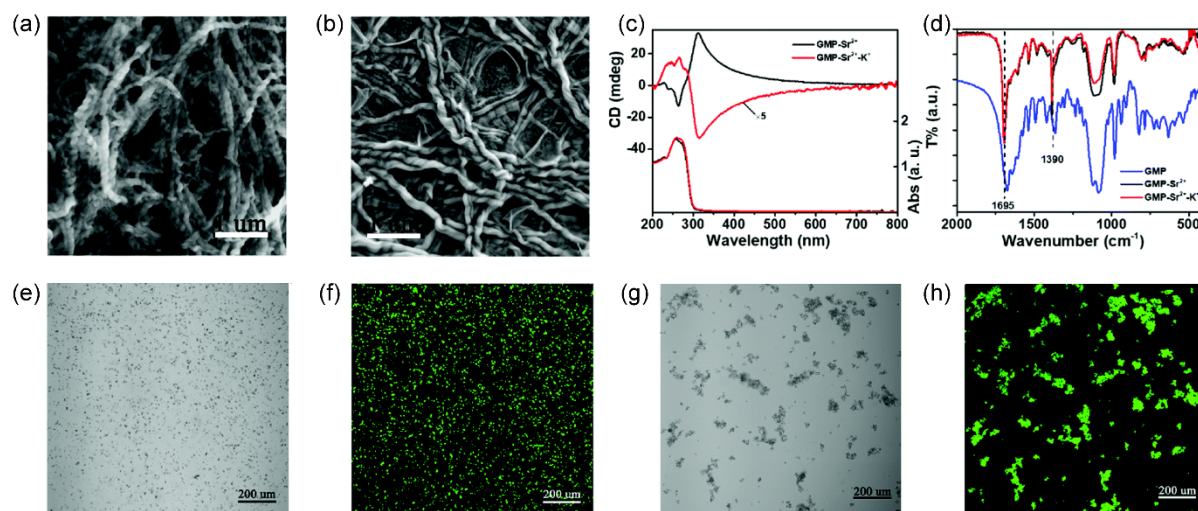


Figure 4 SEM images of (a) $\text{GMP}/\text{Sr}^{2+}$ nanofibers and (b) $\text{GMP}/\text{Sr}^{2+}/\text{K}^+$ nanofibers. (c) CD spectra and (d) FTIR spectra of $\text{GMP}/\text{Sr}^{2+}$ nanofibers and $\text{GMP}/\text{Sr}^{2+}/\text{K}^+$ nanofibers. (e and g) Optical and (f and h) fluorescence microscope images of the complexes of $\text{GMP}/\text{Sr}^{2+}$ and $\text{GMP}/\text{Sr}^{2+}/\text{K}^+$ nanofibers with ThT. Reproduced with permission from ref. [59]. © Royal Society of Chemistry 2020.

inducer. Then, K^+ ions were introduced into the $\text{GMP}/\text{Sr}^{2+}$ self-assembly system to switch the chirality of the fiber. Owing to the predominant chiral environment of the R-/L-hand helical fibers, the R-CPL was successfully obtained by assembling AuAg NCs into the $\text{GMP}/\text{Sr}^{2+}$ nanofibers based on the strong affinity between the NCs

and the fiber. Moreover, the strong CPL emission was used for the detection of L-cysteine with the aggregation-induced quenching by Cys. The synthesis of nanomaterials with metal coordinated nucleotides and their derivatives is summarized in Table 1.

Table 1 Nucleobases and their derivatives for the synthesis of materials.

| Nucleobases and derivatives | Metal ions | Nanomaterials | Ref. |
|--|------------------------------------|-------------------------|------|
| AMP | Au ³⁺ | nanoclusters | [42] |
| AMP | Au ³⁺ | nanoclusters | [43] |
| cAMP | Au ³⁺ | nanoclusters | [44] |
| adenosine, cytidine, or guanosine | Cu ²⁺ | nanoclusters | [45] |
| GMP or GMP | Ag ⁺ | nanoparticles | [49] |
| adenine, cytosine, guanine, or thymine | Ag ⁺ , Au ³⁺ | Au or Ag nanoparticles | [60] |
| AMP | Ag ⁺ , Au ³⁺ | bimetallic nanoclusters | [50] |
| AMP | Ag ⁺ , Au ³⁺ | bimetallic nanoclusters | [51] |
| GMP | Eu ³⁺ | nanoparticles | [61] |
| cytidine | Ag ⁺ | hydrogels | [52] |
| thymine or uracil | Cd ²⁺ | hydrogels | [53] |
| cytosine or guanine | Zn ⁺ | hydrogels | [54] |
| IMP | Ag ⁺ | hydrogels | [62] |
| GMP | Fe ³⁺ | hydrogels | [63] |
| AMP | Mn ²⁺ | hydrogels | [55] |
| GMP | Sr ²⁺ | fibers | [59] |
| GMP | Sr ²⁺ | fibers | [64] |
| adenine | Ag ⁺ | fibers | [65] |

3.4 DNA-coordinated nanomaterials

While the majority of previous work was focused on nucleotide monomers, Li's group recently described the synthesis of nanometer-sized DNA-based materials via coordination-driven self-assembly (Fig. 5) [66]. A one-pot reaction of Fe²⁺ and DNA at 95 °C enabled the production of monodisperse nanospheres with a high yield. The concentrations of Fe²⁺ and DNA in the reaction mixture were important for controlling the size of the Fe-DNA NPs, where higher concentrations resulted in larger NPs. A20 and C20 DNA (20-mer poly-A and poly-C sequences) could generate nanospheres with a size of 213 ± 22 and 71 ± 10 nm, respectively. G20 DNA formed hybrid nanofibers with a diameter of 11-25 nm and a length of 225-455 nm, while T20 failed to form any product. Oligomers of G are known to form G-quadruplex structures that may be responsible for the formation of the nanofibers. The effect of using two types of bases in the same DNA strand was also investigated. When A was combined with T, nanospheres were also obtained, similar to that of A alone. Increasing the number of A base facilitated a higher DNA loading efficiency and the growth of spheres of larger sizes. Hybrid NPs synthesized with DNA consisting of G and A were also nanospheres, confirming the dominating effect of adenine base in the morphology of the final products when combined with other bases. The same group also synthesized a uniform coordination NPs through one-pot supramolecular self-assembly of nucleic acid therapeutics (G3139), doxorubicin (DOX), and Fe²⁺ ions at molar ratio of 1:40:14.5 at 95°C for 1 h [67]. DOX and G3139 not only served as cargos but also participated in the assembly of the NPs through cooperative interactions. Fe-G (the Fe-G3139 NPs without DOX) and DOX/Fe-G were stable in water or HEPES buffer, but

decomposed in PBS buffer due to the competitive coordination of phosphate ions with Fe²⁺ ions. Based on the metal-DNA coordination and hybridization chain reaction amplification strategy, the nanowire balls were synthesized via a one-pot reaction of DNA molecules and Zn²⁺ ions [68].

Aside from random assembly, DNA can also be first made into well-defined nanostructures to form a framework, upon which-templated nanofabrication or mineralization can take place [69]. For example, the Fan group prepared a DNA origami framework, and used it for calcium phosphate (CaP) mineralization with predicted nanostructures due to the inherent affinity of DNA phosphate backbone to Ca²⁺ and the programmability of DNA [70]. The spontaneous formation of hybrid nanomaterials through biomineralization of Y-shaped DNA and Cu²⁺ ions was reported [71], where the nitrogen bases and sugar-phosphate backbone of the Y-DNA played an important role in mediating the biomineralization. They would interact with Cu²⁺ ions through electrostatic and coordination interactions. Initially, the Y-DNA would form complexes with Cu²⁺ ions to provide the nucleation sites and then form the primary crystals. Increasing the reaction time, larger agglomerates of the primary crystals formed and gradually grew into 3D hierarchical flowers consisted of the closely packed nanoplates. Replacing Cu²⁺ with Ca²⁺, the 3D hierarchical particles consisting of coupled irregular nanoplates were obtained with the Y-DNA. Khalifehzadeh et al. also revealed that the characteristics of CaP are highly dependent on the composition, backbone, sequence and concentrations of oligonucleotide molecules [72]. CaP mineralization was blocked when the concentration of phosphodiester was over a certain range, while this effect was not observed for the increased concentration of phosphorothioate groups.

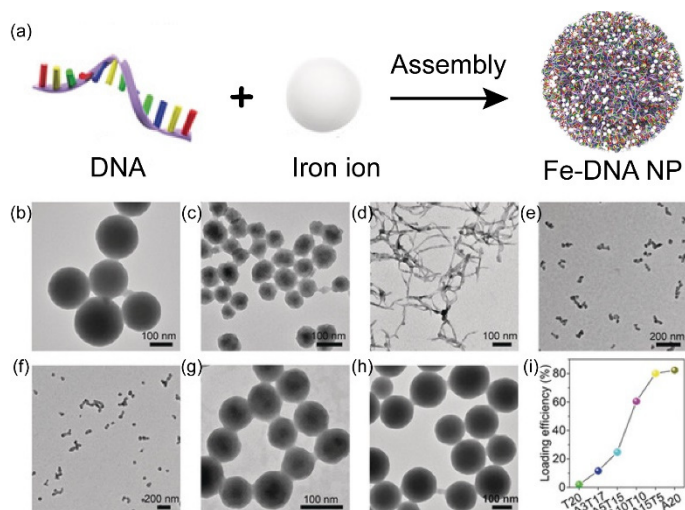


Figure 5 Coordination-driven self-assembly of Fe^{2+} and DNA for cancer therapy. (a) Scheme of the assembly of Fe-DNA nanoparticles. TEM images of the Fe-DNA nanoparticles synthesized with (b) A20, (c) C20, (d) G20, (e) A3T17, (f) A5T15, (g) A10T10, and (h) A15T5. (i) DNA loading efficiency of Fe-DNA nanoparticles. Reproduced with permission from ref. [66]. © Wiley-VCH Verlag GmbH & Co. KGaA, Weinheim 2019.

Kim et al. demonstrated that covalent attachment of polyaspartic acid to DNA nanotubes influenced both the organization of amorphous CaP, and the morphology of the growing minerals across multiple length scales [70]. These results offer new insight into the control of calcium phosphate mineralization in the presence of various derivatives of nucleic acids. Recently, Li et al. studied the optical properties of DNA coordinated Yb^{3+} nanomaterials [73]. The DNA increased the luminescence of Yb^{3+} complexes. On the basis of direct quenching effects of Cu^{2+} and Fe^{3+} , these nanomaterials were used to detect Cu^{2+} and Fe^{3+} in vitro and in vivo.

DNA coordination is also useful for the surface functionality of metal-organic frameworks (MOFs). A typical example is the Zr-based MOF that shows a high affinity toward phosphate groups (PO_4^{3-}) through the strong coordination between phosphate and zirconium. The Mirkin group developed a coordination chemistry-based strategy for the surface functionalization of the external metal nodes of UIO-66 nanoparticles with PO_4^{3-} -terminated DNA [74, 75]. By taking advantage of the programmable and specific interactions of DNA, MOF particle-inorganic particle core-satellite hybrids were synthesized. The DNA-rich surfaces made MOFs stable and ensure facile cellular entry. Fan and coworkers also demonstrated that DNA can stably adsorb on UIO-66 by the formation of Zr-O-P bonds [76]. Surface-bound DNA can be efficiently released in either bulk solution or live cells when free PO_4^{3-} are present. Based on this feature, PO_4^{3-} -terminated DNA-functionalized UiO-66 NPs were used to develop sensing and imaging systems [77-80]. Moreover, using Zr-based porphyrinic MOF (ZrMOF) nanoparticles as photosensitizers and aptamers as targeting ligands, phosphate-terminated aptamers anchored on ZrMOF nanoparticles achieved targeted photodynamic therapy effect [81, 82].

4 Applications of nucleotide coordination nanomaterials

A broad range of distinct characteristics of these coordination nanomaterials based on nucleobases and their derivatives endow them with diverse applications in many fields, including biosensing,

enzyme encapsulation, anti-bacteria activities, drug delivery, and cancer therapy. Some representative examples are reviewed in this section.

4.1 Biosensing

These coordination nanomaterials possess adsorption, fluorescence quenching, and light absorption properties, which are useful for biosensor development. Our group studied DNA adsorption and desorption from various Ln^{3+} /nucleotide nanoparticles using AMP and GMP as ligands [83]. The AMP CPs adsorbed DNA more strongly than the GMP ones. Using mixtures of AMP and GMP, continuous tuning of DNA adsorption affinity was achieved. On the basis of the different affinities of single- and double-stranded DNA on CPs, such CPs can be used for DNA sensing (Fig. 6(a)). A detection limit of 0.9 nM target DNA was achieved.

Aside from DNA detection, nucleotide-coordinated nanomaterials were also employed for protein detection, such as alkaline phosphatase (ALP), carcinoembryonic antigen (CEA), and lactate dehydrogenase (LDH). For example, Chen et al. developed a fluorescence assay for ALP detection based on ATP-triggered disassociation and fluorescence quenching of cerium nanoparticles (CPNs) [84]. ATP acted as an “antenna” to sensitize the luminescence of Ce^{3+} with the aid of tris(hydroxymethyl) aminomethane (Tris), forming Ce^{3+} -ATP-Tris CPNs. ATP was catalytically converted into adenosine and inorganic orthophosphate, inducing fluorescence quenching. Taking advantage of the luminescence property of AMP-protected bimetallic nanoclusters (Au-AgNCs@AMP), a LDH sensing platform was established [85]. Very recently, Wu et al. developed a colorimetric immunoassay based on Zn^{2+} /adenine CPs for the detection of CEA (Fig. 6(b)) [86]. Using iron(II)-phenanthroline complexes for signal amplification, a detection limit of 21.1 pg/mL was achieved.

Sensitive detection of metal ions is important in biological and environmental systems. Ungor et al. synthesized AMP-stabilized gold nanoparticles and fluorescent gold nanoclusters [87]. Significant fluorescence quenching of the AuNCs was observed in the presence of Fe^{3+} ions, and a detection limit of 2.0 μM was achieved. Zhan et al. synthesized cytosinetriphosphate (CTP) capped AgNPs by the reduction of AgNO_3 in the presence of CTP [88]. The AgNPs aggregated with the addition of Cr^{3+} , resulting in a color change of the AgNPs from yellow to red. Exposure to Hg^{2+} led to the formation of a mercury layer around the surface of the AgNPs, which faded the yellow color. Taking advantage of the remarkably rapid responses of such AgNPs to Cr^{3+} and Hg^{2+} over other metal ions, a new method for the detection of either Cr^{3+} or Hg^{2+} was developed, with detection limits of 6.25 μM Cr^{3+} and 0.125 μM Hg^{2+} .

Some small biomolecules such as cysteine (Cys), glutathione (GSH), glucose and inorganic phosphate are important physiological indicators. Zhang et al. found the quenching effect of Cys to the fluorescence of AMP-capped bimetallic gold and silver nanoclusters (AuAgNC@AMP) [89]. Using this effect, a sensor for Cys was developed. In another work, gold/silver nanoclusters with yellow fluorescence were synthesized for Cys and GSH detection because of their quenching effect [90]. Tan et al. fabricated a fluorescent nanoprobe with Tb^{3+} as a metal node, ATP as a bridge ligand, and carboxyphenylboronic acid as a sensitizer in which superoxide dismutase is encapsulated by a self-adaptive inclusion process [91]. Superoxide dismutase can convert superoxide anions into H_2O_2 to induce the deboronation of carboxyphenylboronic acid, resulting in

the quenched fluorescence of the nanoprobe. Based on this finding, a fluorescence method for superoxide anions detection was proposed. Since CPs can entrap enzymes, such as glucose oxidase (GOx) and horseradish peroxidase (HRP), several glucose sensors have been reported [92-96].

Phosphate (Pi) plays important roles in various physiological processes, including cellular signaling and cell growth. Therefore, an accurate determination of phosphate is very important. Zhao et al. designed a facile fluorescent sensor for Pi measurement with an europium (Eu)-based CP nanoprobe (Eu/DPA/Ade), which was formed by coordinating 2,6-pyridinedicarboxylic acid (2,6-DPA) and adenine (Ade) with Eu^{3+} (Fig. 6(c)) [97].

Monitoring toxic and harmful chemicals has also attracted extensive attention. 2,4,6-trinitrophenol (TNP) is widely used in both military and commercial affairs because of its explosive power. The broad application of TNP has drawn increasing interest in its detection. Gao et al. designed fluorescent CPs derived from GMP and Tb^{3+} ions, whose fluorescence could be specifically decreased by TNP via photo-induced charge transfer. As a result, the CPs were applied for TNP detection [98]. The antibiotic oxytetracycline (OTC) is widely used as food additives on cows feeding and then may be

found as a residue in the dairy products, which have increased demand for accurate, sensitive, and selective determination methods for OTC in milk. Chen et al. designed a ratiometric sensor for OTC detection based on AMP/ Eu^{3+} CPs doped with carbon dots (CDs) [102]. The CD@AMP/ $\text{Eu}(\text{III})$ CPs were fabricated by self-assembly of Eu^{3+} ions and AMP on the surface of CDs. The AMP/ Eu^{3+} moiety was used as a probe, while the CDs served as a reference for providing built-in corrections to correct for environmental effects. The sensors based on nucleotides and DNA coordinated metal ions are summarized in Table 2. A wide variety of target analytes are listed, including DNA, proteins, metal ions and small molecules.

4.2 Enzyme encapsulation

Enzymes are mainly protein-based biocatalysts with excellent activity and specificity, but their applications are limited due to high cost, short lifetime, and low operational stability [103, 104]. Since nucleotide/metal CPs are typically formed by a simple mixing step at room temperature and have a porous structure, they could act as favorable biocatalyst supports for enzyme immobilization.

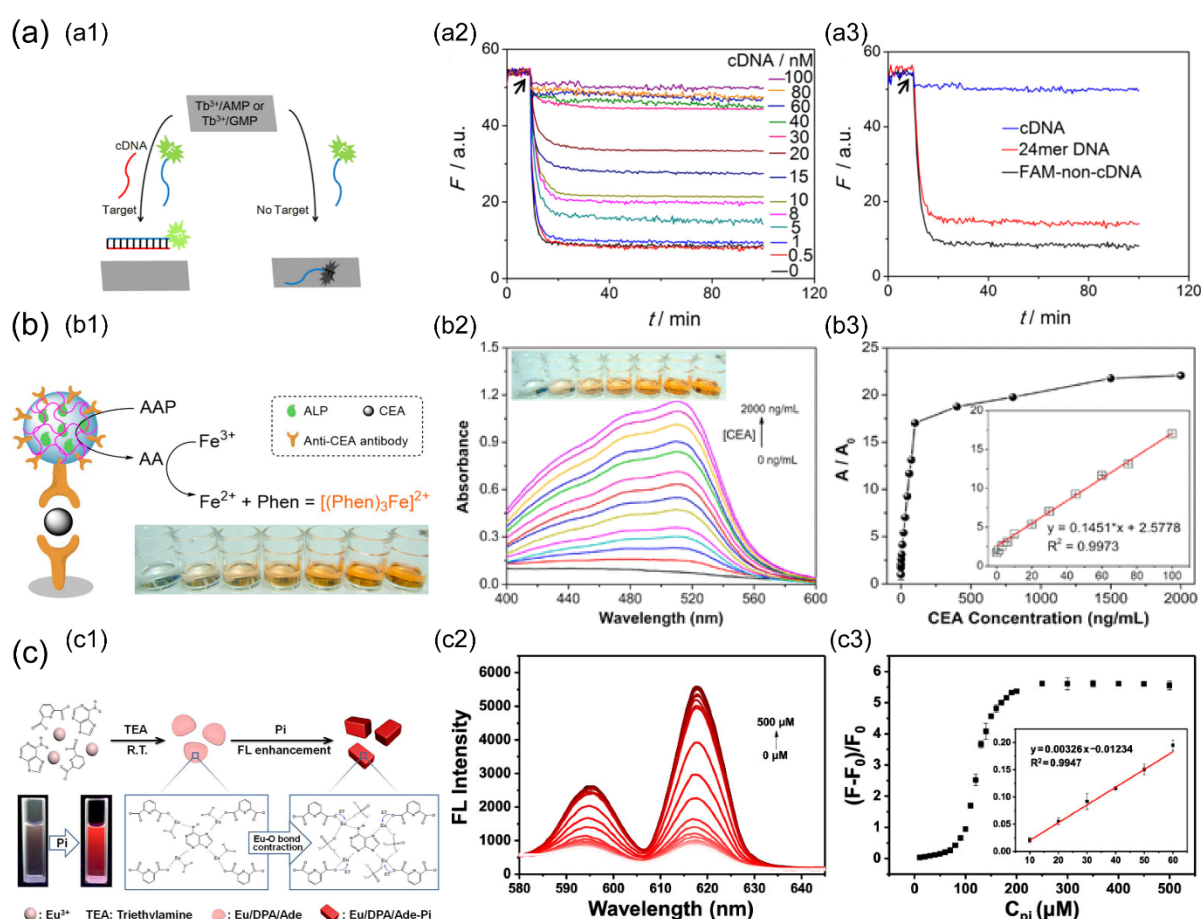


Figure 6 (a) Adsorption of FAM-labeled DNA on Tb^{3+} /AMP or Tb^{3+} /GMP for DNA detection. (a1) Schematics of DNA sensing based on the DNA adsorption. (a2) Kinetics of FAM-24-mer DNA adsorption by Tb^{3+} /GMP versus cDNA. (a3) Kinetics of the free FAM-24-mer DNA adsorption by Tb^{3+} /GMP, with a 24-mer non-target DNA, and with the target cDNA, respectively. Reprinted with permission from ref. [83]. © American Chemical Society 2018. (b) Colorimetric immunoassay based on adenine coordinated nanoparticles for CEA detection. (b1) Scheme of the colorimetric immunoassay. Absorption spectra (b2) and intensities (b3) of $[(\text{Phen})_3\text{Fe}]^{2+}$ complex produced in the immunoassays toward various concentrations of CEA. Reprinted with permission from ref. [86]. © American Chemical Society 2019. (c) Europium-pyridinedicarboxylate-adenine fluorescence nanoprobe for phosphate detection. (c1) Schematic illustration of Eu/DPA/Ade fluorescence nanoprobe for phosphate detection. (c2) Fluorescence spectra of the Eu/DPA/Ade nanoprobe at various concentrations of phosphate. (c3) Relationship between the fluorescence ratio

and phosphate concentration. Reprinted with permission from ref. [97]. © American Chemical Society 2020.

Table 2 The sensors and biosensors based on the coordination between nucleotide/DNA and metal ions.

| Nucleotide/DNA | Metal ion | Analyte | Limit of detection | Ref. |
|----------------|------------------------------------|--|---|-------|
| DNA | Cu ²⁺ | mRNA | 0.56 nM | [71] |
| GMP | Tb ³⁺ | DNA | 0.9 nM | [83] |
| adenine | Au ³⁺ | ALP | 0.003 U/L | [99] |
| ATP | Ce ³⁺ | ALP | 0.09 U/L | [84] |
| AMP | Ag ⁺ , Au ³⁺ | Plasmodium vivax lactate dehydrogenase | 0.1 nM | [85] |
| adenine | Zn ²⁺ | CEA | 21.1 pg/mL | [86] |
| DNA | Yb ³⁺ | Cu ²⁺ ; Fe ³⁺ | — | [73] |
| AMP | Au ³⁺ | Fe ³⁺ | 2 μM | [87] |
| ATP | Tb ³⁺ | Fe ²⁺ | 20 nM | [100] |
| CTP | Ag ⁺ | Hg ²⁺ ; Cr ³⁺ | Hg ²⁺ : 0.125 μM; Cr ³⁺ : 6.25 μM | [88] |
| GMP | Ag ⁺ | GSH | 1.03 μM | [49] |
| AXP | Au ³⁺ | GSH | 20 μM | [101] |
| AMP | Ag ⁺ , Au ³⁺ | Cys | 95.7 nM | [64] |
| AMP | Ag ⁺ , Au ³⁺ | Cys | 50 nM | [89] |
| cytidine | Ag ⁺ , Au ³⁺ | Cys; GSH | Cys: 0.74 nM GSH: 5 μM | [90] |
| AMP | Fe ³⁺ | glucose | 1.4 μM | [92] |
| adenine | Zn ²⁺ | glucose | 1.84 μM | [94] |
| AMP | Tb ³⁺ | glucose | 80 nM | [95] |
| AMP | Zn ²⁺ | glucose | 0.3 μM | [96] |
| GMP | Cu ²⁺ | glucose | 0.3 mM | [93] |
| adenine | Eu ³⁺ | phosphate | 4.65 μM | [97] |
| GMP | Tb ³⁺ | 2,4,6-trinitrophenol | 26 nM | [98] |
| AMP | Eu ³⁺ | oxytetracycline | 0.5 μM | [102] |

The immobilized enzymes can preserve or even improve their activity on solid supports [105]. Recently Liang et al. reported that a CP generated from adenine and Zn²⁺ enhanced the activity and stability of encapsulated methionine adenosyltransferase (MAT) (Fig. 7) [106]. This was attributable to the coordination of Zn²⁺ and adenine around the surface of the enzyme, confining its structure change. Later, the same group reported acid-stable Zr⁴⁺/AMP CPs for efficiently improving acidophilic enzymes immobilization [107]. Lou et al. reported Cu²⁺ coordinated CMP encapsulated lipase composites via in-situ assembly [108].

In addition to using single enzymes, co-immobilization of multiple enzymes in CPs was also demonstrated. Our group co-immobilized GOx and HRP in Zn²⁺/AMP hydrogels [96]. The hydrogel not only had a high enzyme encapsulation capacity, but also improved the stability of the entrapped enzymes against extreme pH, temperature variation and long-term storage. The enzymes retained higher activity in the hydrogels compared to that in the more rigid

nanoparticles formed with AMP and lanthanide ions [27]. Liang and coworkers also reported co-immobilization of GOx and HRP in Cu/GMP matrix [93], where the enzyme stability was increased by 40% at pH 3 and the thermal stability was increased by more than 70% at 90°C. The storage stability was also 8 times higher than the free enzymes after thirteen days.

CPs were also used for co-immobilization of enzymes and nanoparticles to prepare multifunctional composites. Liang and coworkers demonstrated the co-immobilization of candida rugosa lipase (CRL) and Fe₃O₄ nanoparticles in Zn²⁺/AMP [109]. The immobilized CRL had high reusability and excellent long-term storage stability due to the Fe₃O₄@Zn/AMP hydrogels protecting CRL from harsh conditions. Tan et al. reported that the self-assembly of Tb³⁺, AMP, GOx and CDs led to the formation of GOx&CDs@AMP/Tb composites with catalytic and fluorescence properties [95]. This composite displayed about 2-fold higher catalytic activity than free GOx. Benefiting from the synergistic

effect of GOx and CDs in the highly efficient transfer of intermediates and the elimination of environmental fluctuations, this composite was used to fabricate a highly sensitive sensor for

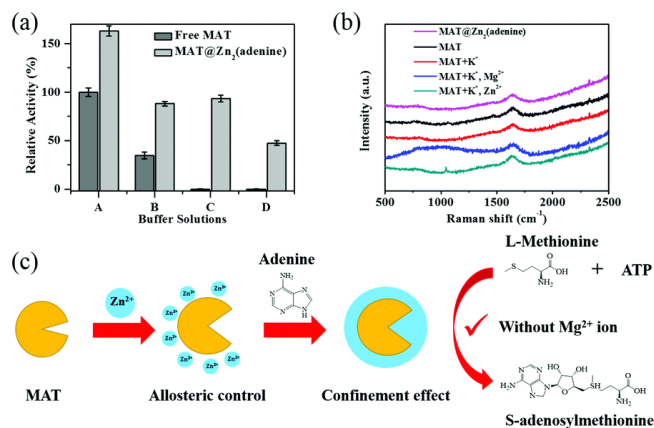


Figure 7 (a) The relative activity of the immobilized MAT enzyme by Zn₂(adenine) nanoparticles compared to the free MAT with adding different metal ions in reaction buffer. (b) Raman spectrum of MAT with different metal ions and MAT@Zn₂(adenine) in the 500–2500 cm⁻¹ region. (c) Schematic illustration of the immobilization of MAT by Zn₂(adenine). Reprinted with permission from ref. [106]. © Royal Society of Chemistry 2019.

4.3 Nanozymes

Nanozymes refer to nanomaterials with enzyme-like activities [110–113]. Compared to natural enzymes, nanozymes have the advantages of higher stability and lower cost. Some CPs have enzyme-like activities and thus they belong to the nanozyme family [112–114]. Our group compared the CPs formed by adenine, 2-aminopurine (2AP) and adenosine with various metals [115]. Only Au³⁺ produced CP nanoparticles with both adenine and 2AP. The 2AP-Au and adenine-Au exhibited oxidase-like activity for TMB oxidation possibly by the Au³⁺ exposed on the surface. Wu et al. prepared GMP-protected bimetallic nanoclusters of gold and platinum (Au–PtNCs-GMP) for oxidase-like catalysis [116]. The synergistic effect of Au and Pt atoms endowed Au–PtNCs-GMP with high catalytic activity, which opens a way for the development of other oxidase-mimicking nanozymes.

Cu²⁺ ions were also used to fabricate nanozymes via coordination interactions. Our group found that Cu²⁺-catalyzed TMB oxidation can be greatly accelerated with excess nucleotides and nucleosides [117]. Notably, GMP exhibited the best activity through the formation of coordination nanozymes, which can be attributed to the specific binding between the electron-rich oxygen and nitrogen atoms of guanine with Cu²⁺.

Overall, the activity followed the order: GMP > guanosine > cytidine > AMP ≈ CMP > adenosine. Binding of Cu²⁺ in the porous coordination nanozyme structure of Cu²⁺/GMP allowed the accessibility of Cu²⁺ for the catalytic reaction. In another work, our group reported a laccase mimicking nanozyme based on GMP coordinated copper [118]. The activity was derived from guanosine coordination rather than phosphate binding in GMP. Cu²⁺ was essential and cannot be replaced by other metal ions. To achieve the same catalytic efficiency, the cost of the Gu/GMP was ~2400-fold lower than that of laccase.

glucose detection.

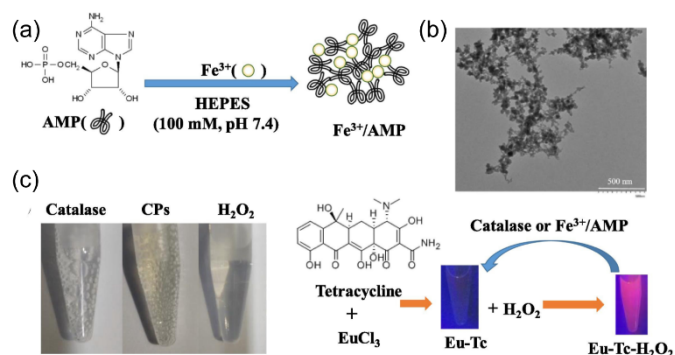


Figure 8 (a) Scheme of mixing Fe³⁺ with AMP to form the CPs. (b) A TEM image of the Fe³⁺/AMP CPs. (c) The photos showing oxygen bubbles due to the activity of catalase, the Fe³⁺/AMP CPs and a blank control with 0.3% H₂O₂. (d) The mechanism of fluorescence-based detection of H₂O₂ by europium (III)-tetracycline (Eu-Tc). Reproduced with permission from ref. [119]. © Elsevier 2020.

Iron ions were also used to prepare CP nanozymes. Recently, a catalase-mimicking Fe³⁺/AMP coordination nanoparticle was reported (Fig. 8) [119]. This nanoparticle also displayed peroxidase-like activity in acidic pH, but catalase-like activity at neutral pH. The nanozyme was much more robust than natural catalase under harsher conditions. Co-immobilization of glycolic acid oxidase and Fe³⁺/AMP in nanogels resulted in an enzyme cascade system using glycolic acid as a substrate, which solved the problem of enzyme deactivation by the accumulated H₂O₂ by-product. The nanozyme was further encapsulated in nanogels, which greatly improved the catalytic activity, substrate tolerance and reusability of co-immobilized catalysts due to its confinement and protection effect.

Noble metals such as Pt and Pd have drawn much attention due to their excellent catalytic properties. Fu's group used CMP, TMP, GMP and AMP, respectively, to modulate the coordination environment of PtCl₄²⁻ [120]. They found that these four nucleotides had the ability to generate Pt nanoclusters with peroxidase-like activity. The nucleotides served as both reducing agents and stabilizers in the formation of the Pt nanoclusters. Both the particle size and the valence state of Pt nanoclusters were associated with the chemical structures of nucleotides. X-ray photoelectron spectroscopy (XPS) demonstrated that the Pt⁰ and Pt²⁺ species were produced during the formation of Pt nanoclusters. The presence of Pt⁰ might contribute to their enzyme-like activity. Zou et al. used GTP, GDP, GMP, CMP and TMP, respectively, to prepare Pd nanocatalysts, where the nucleotides served as electron donors and stabilizers [121]. The catalytic property of the Pd nanocatalysts varied significantly with the chemical structures of nucleobases as well as the number of phosphate groups. The Pd-GTP possessed high catalytic activity in the hydrogenation reduction of 4-nitrophenol assisted by NaBH₄. This is a green and facile strategy to prepare Pd-based nanocatalysts.

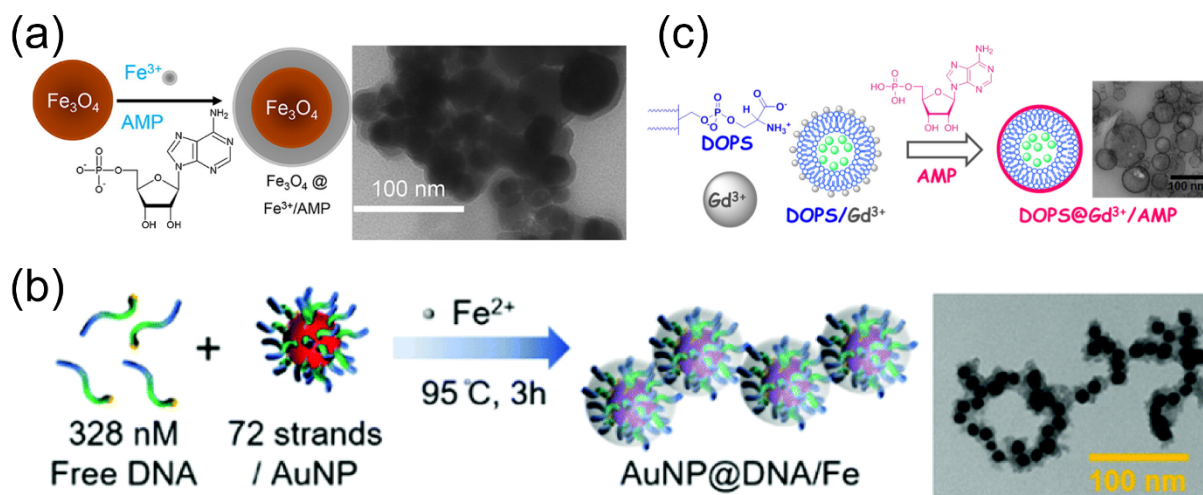


Figure 9 (a) Scheme of seeded growth of $\text{Fe}^{3+}/\text{AMP}$ CPs around Fe_3O_4 NPs and TEM image of $\text{Fe}_3\text{O}_4 @ \text{Fe}^{3+}/\text{AMP}$. Reproduced from ref. [92]. © American Chemical Society 2016. (c) Scheme and TEM image showing the products synthesized with $\text{AuNP}@DNA$ with free DNA. Reproduced from ref. [122]. © Royal Society of Chemistry 2020. (c) Scheme and TEM image of formation of $\text{DOPS}@Gd^{3+}/\text{AMP}$. Reproduced with permission from ref. [123]. © American Chemical Society 2019.

In addition, nucleotides could also act as a promoter to improve the catalytic activity of nanozymes. Tseng's group demonstrated that adenosine nucleotides were capable of improving the peroxidase-like activity of Fe_3O_4 NPs using amplex ultrared as a substrate [124]. Such enhancement was attributed to the coordination between nucleotides and the $\text{Fe}^{2+}/\text{Fe}^{3+}$ sites on the surface of the Fe_3O_4 NPs. AMP might serve a role similar to the distal histidine residue of HRP for activating H_2O_2 bound to $\text{Fe}^{2+}/\text{Fe}^{3+}$ sites. The order of adenosine analogs in increasing the peroxidase-like activity of Fe_3O_4 NPs was $\text{AMP} > \text{ADP} > \text{ATP}$, which might result from the different adsorption efficiency of these nucleotides. In a later work, the same group found that the peroxidase-like activity of citrate-stabilized AuNPs, citrate-capped PtNPs, bovine serum albumin-encapsulated AuNCs, and unmodified Fe_3O_4 NPs was significantly improved in H_2O_2 -induced oxidation of amplex ultrared upon the addition of adenosine-related compounds [125]. This observation offered a general method for exploration of adenosine analogues as a promoter for various peroxidase-like biocatalysts.

4.4 Surface modification

The modification of functional molecules on the surface of nanoparticle cores is of great importance. Although a lot of efforts have been devoted to incorporate guest molecules/materials onto particle surfaces [126-131], most of them require multiple synthetic manipulations. Coordination-mediated surface functionalization of particles with CPs is a simple, mild and efficient strategy. Liang et al. demonstrated the growth of a polymer shell made of AMP and Fe^{3+} on magnetic Fe_3O_4 nanoparticles (Fig. 9(a)) [92]. The shell could further entrap a diverse range of guest molecules, including small molecule fluorophores, proteins, DNA, and AuNPs and increase the peroxidase-like activity of the Fe_3O_4 core. All of these guests were loaded with better stability compared to that on the naked Fe_3O_4 NPs, confirming the advantage of the CP shell. With entrapped GOx, an enzyme cascade reaction was realized by relaying the GOx and HRP

mimicking activities, which could be used for glucose detection. This study provided a simple and facile strategy to fabricate hybrid nanomaterials. Later, a Cu/GMP nanozyme shell was also constructed on the surface of magnetic Fe_3O_4 core with excellent laccase-like activity, outstanding environmental tolerance and high stability [132]. Aside from iron oxide, a CP shell was also formed on bare AuNPs [133], DNA-functionalized AuNPs [122], QDs [134] and liposomes [123].

Very recently, our group reported the growth of a DNA/Fe shell with controllable thickness on DNA-functionalized AuNPs (Fig. 9(b)) [122]. Taking advantage of the high local DNA density, the required DNA concentration decreased from micromolar to nanomolar levels (free DNA in solution also required). The ratio of DNA and Fe^{2+} determined the final morphology of $\text{AuNP}@DNA/\text{Fe}$ core-shell structures. A higher DNA concentration not only led to a thicker shell on the AuNPs but also prevented the aggregation of the AuNPs. Owing to the selective etching of DNA/Fe shell by the competitive molecules, such as phosphate, $\text{AuNP}@DNA/\text{Fe}$ can be applied for drug delivery and colorimetric sensing. For QDs, Nishiyabu et al. concluded that self-assembly of nucleotides and lanthanide ions in water selectively occurred on the surface of carboxyl-QDs, leading to the formation of core-shell nanostructures [134]. The thickness of the coordination shell was tunable depending on the concentration of the QDs employed. A broad range of nucleotides and lanthanide ions could be wrapped on the surface of the anionic QDs to grow coordination network shells.

Liposomes might also direct the growth of coordination materials due to their metal coordination ligands such as phosphate of many lipids. Our group reported that a gadolinium/AMP (Gd^{3+}/AMP) shell was formed on liposomes by a simple mixing (Fig. 9(c)) [119], which protected the liposomes from leakage by nanoparticles. Apart from the seeded growth of a CP shell, individual nucleotides without metal ions coordination can also form a thin layer on AuNPs [131, 132], gold nanoflowers [133], AgNPs [134, 135], and QDs [136, 137].

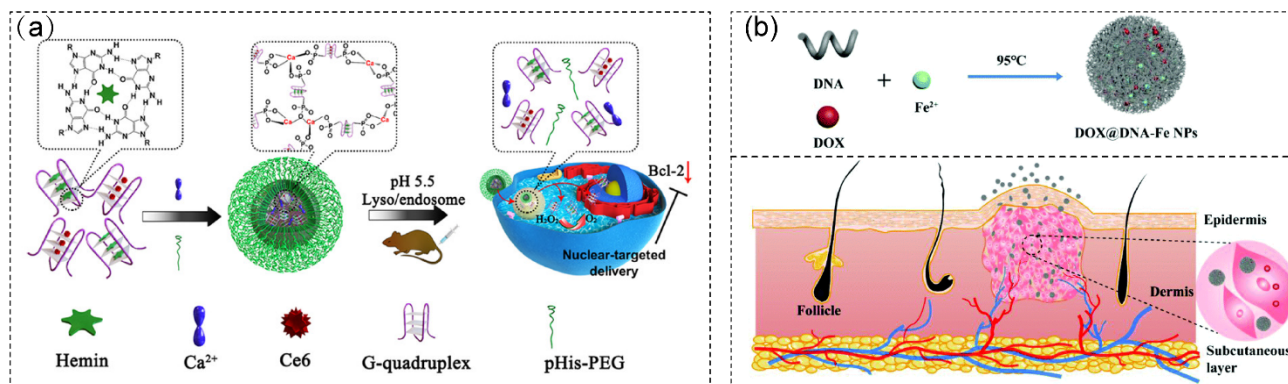


Figure 10 (a) Schematic illustration for synthesis of CACH-PEG and its application for targeted cancer therapy. Reproduced with permission from ref. [135]. © American Chemical Society 2018. (b) Preparation process of DOX@DNA-Fe NPs and their application in hypertrophic scar therapy. Reproduced with permission from ref. [136]. © Royal Society of Chemistry 2020

4.5 Biomedical applications

The tunable size, excellent biocompatibility, and stable optical properties of nucleobase-templated architectures have also attracted much attention in biomedical fields. Spontaneous formation of hydrogels by mixing Ag⁺ ions and i-motif DNA and its boronate ester derivatives was reported [137]. Base-pairing interactions between free cytidine and cytidine-boronate esters as well as π - π stacking interactions of aryl rings were presumed to be the determining factors for the supramolecular architecture. These hydrogels showed potent antibacterial activities due to the silver ions, and their selectivity toward Gram-negative bacteria was enhanced by altering their boronic acid component.

Coordination-driven self-assembly of metal ions and nucleobases or its derivatives could be used to deliver nucleic acids to cells. Li et al. described the synthesis of nanometer-sized DNA materials for DNA delivery via coordination-driven self-assembly of Fe²⁺ ions and DNA [66]. Fe-DNA nanoparticles of precise sizes and controlled compositions can be produced. The obtained nanoparticles were utilized to deliver an immunostimulatory DNA, CpGs, to cells in vitro and in vivo with enhanced biological functions. The Fe-CpG NPs exhibited higher cellular uptake, immunoactivation efficiency, and antitumor effect than the free CpG. The significant antitumor activity of Fe-CpG NPs might result from a combination of nanoscale effects, the high cellular uptake capability, improved stability of loaded CpG, and increased tumoral accumulation due to the enhanced permeability and retention (EPR) effect.

Besides DNA delivery, drug delivery and controlled release is another important application of self-assembled DNA and metal ions. Zhang et al. reported metal ion-assisted assembly of DNA-minocycline complexes for controlled minocycline release [138]. In the presence of Mg²⁺ or Ca²⁺, minocycline could bind to the phosphate backbone of DNA via an electrostatic bridge of metal ions to form aggregated particles. The complexes could prolong minocycline release from agarose gel to more than 10 days as compared to the quick release of free minocycline from the gel within 1 day. The released minocycline from the complexes retained the anti-inflammatory bioactivity to inhibit nitric oxide production from pro-inflammatory macrophages. Co-delivery of nucleic acids and drugs were also investigated due to their synergistic effects. Liu's group designed a DNA nanostructure based on the coordination between Ca²⁺ and AS1411 DNA G-quadruplex to form nanoscale

CPs [135]. Both chlorine e6(Ce6), a photosensitizer, and hemin, an iron-containing porphyrin, can be loaded into the G-quadruplex structure in the CPs (Fig. 10(a)). With further polyethylene glycol (PEG) modification, a nanoscale drug-delivery system was fabricated, which improved cancer therapy. Li's group developed a biomimetic nanoplatform for systemic codelivery through one-pot supramolecular self-assembly of a DNA therapeutic agent (G3139), a chemotherapeutic drug doxorubicin (DOX), and Fe²⁺ ions via multiple coordination interactions [67]. The DOX/Fe was then mineralized with a thin shell of ZIF-8 MOF to yield the final core-shell structured nanoplatform, which achieved efficient co-delivery and effectively suppressed tumor growth, allowing for sensitive MRI detection and synergistic gene therapy and chemotherapy. Recently, Jiang et al. employed a DNA-Fe nanoparticle delivery system via Fe²⁺ driven self-assembly for hypertrophic scars (HSs) therapy (Fig. 10(b)) [136]. DOX was employed to treat the hyperplasia of abnormal skin fibrous tissues. Both in vitro and in vivo experiments of the DOX-loaded DNA-Fe nanoparticles demonstrated penetration ability, rapid drug release, and scar-inhibiting effects.

5 Conclusions and perspectives

In this review, we summarized recent advances of nucleobase, nucleoside, nucleotide and DNA oligonucleotide coordinated metal ion complexes, which can form a wide range of interesting materials including nanoparticles, luminescent nanoclusters, fibers, and hydrogels. The size, morphology, and properties of the final materials can be tuned by changing the composition of the nucleotides and metals. The diverse optical, physical and catalytic properties of the materials endow them with different functions. The obtained nanomaterials have been used in biosensing, enzyme encapsulation, catalysis, cellular imaging, and cancer therapy. With numerous advances achieved, some challenges of this field need to be addressed in future work.

(1) The type of nucleotides used as templates to prepare the coordination complexes is limited. The lack of functional groups, such as the thiol or carboxylate groups, limits their further modification. It is important to expand the chemical functionality of the building blocks and it could be interesting to use both nucleotides and amino acids as ligands. Synthetic chemistry can also be used to rationally synthesize new ligands based on the nucleotide structures. (2) From the functional aspects, it would be interesting to achieve stimuli-responsive structures, dynamic assembly, and

programmable production. (3) Although nucleotide/DNA-based materials have shown great potential in bio-related applications, certain challenges still need to be addressed. For example, the active targeting capability, the appropriate circulation time, long-term toxicity in living organism, active/passive accumulation effect, tissue biodistribution are essential issues for their biomedical applications. The studies may bring novel insights for designing bio-safe nanomedicines. In particular, stability against phosphate is an important issue since phosphate may compete with nucleotides or DNA and disrupt the structures. (4) Aside from the fluorescence signals, the electrochemical, electrochemiluminescent or photoelectrochemical properties of nucleotide-templated nanomaterials are hardly explored to construct sensors. The use of these properties will dramatically extend their biosensing applications. In addition, the prepared nanomaterials should be simple, cost-effective, stable, and controllable.

Acknowledgements

We gratefully appreciate the support from Natural Sciences and Engineering Research Council of Canada (NSERC), and National Natural Science Foundation of China (21778020). J. Zhou was supported by the HZAU overseas Academic Fund to visit the University of Waterloo.

References

- [1] Dann III, C. E.; Wakeman, C. A.; Sieling, C. L.; Baker, S. C.; Irnov, I.; Winkler, W. C. Structure and mechanism of a metal-sensing regulatory RNA. *Cell* **2007**, *130*, 878-892.
- [2] Waldron, K. J.; Rutherford, J. C.; Ford, D.; Robinson, N. J. Metalloproteins and metal sensing. *Nature* **2009**, *460*, 823-830.
- [3] Wang, J.; Luo, C.; Shan, C.; You, Q.; Lu, J.; Elf, S.; Zhou, Y.; Wen, Y.; Vinkenborg, J. L.; Fan, J. Inhibition of human copper trafficking by a small molecule significantly attenuates cancer cell proliferation. *Nat. Chem.* **2015**, *7*, 968.
- [4] Outten, C. E.; O'Halloran, T. V. Femtomolar sensitivity of metalloregulatory proteins controlling zinc homeostasis. *Science* **2001**, *292*, 2488-2492.
- [5] Zahir, F.; Rizwi, S. J.; Haq, S. K.; Khan, R. H. Low dose mercury toxicity and human health. *Environ. Toxicol. Pharmacol.* **2005**, *20*, 351-360.
- [6] Wang, H.; Kim, Y.; Liu, H.; Zhu, Z.; Bamrungsap, S.; Tan, W. Engineering a unimolecular DNA-catalytic probe for single lead ion monitoring. *J. Am. Chem. Soc.* **2009**, *131*, 8221-8226.
- [7] Tan, S. S.; Teo, Y. N.; Kool, E. T. Selective sensor for silver ions built from polyfluorophores on a DNA backbone. *Org. Lett.* **2010**, *12*, 4820-4823.
- [8] Tchounwou, P. B.; Ayensu, W. K.; Ninashvili, N.; Sutton, D. Environmental exposure to mercury and its toxicopathologic implications for public health. *Environ. Toxicol.* **2003**, *18*, 149-175.
- [9] Lake, R. J.; Yang, Z.; Zhang, J.; Lu, Y. DNazymes as activity-based sensors for metal ions: recent applications, demonstrated advantages, current challenges, and future directions. *Accounts Chem. Res.* **2019**, *52*, 3275-3286.
- [10] Sigel, R. K.; Sigel, H. A stability concept for metal ion coordination to single-stranded nucleic acids and affinities of individual sites. *Acc. Chem. Res.* **2010**, *43*, 974-984.
- [11] Zhou, W.; Saran, R.; Liu, J. Metal sensing by DNA. *Chem. Rev.* **2017**, *117*, 8272-8325.
- [12] Ward, W. L.; Plakos, K.; DeRose, V. J. Nucleic acid catalysis: metals, nucleobases, and other cofactors. *Chem. Rev.* **2014**, *114*, 4318-4342.
- [13] Lopez, A.; Liu, J. Self-assembly of nucleobase, nucleoside and nucleotide coordination polymers: from synthesis to applications. *ChemNanoMat* **2017**, *3*, 670-684.
- [14] He, Y.; Lopez, A.; Zhang, Z.; Chen, D.; Yang, R.; Liu, J. Nucleotide and DNA coordinated lanthanides: From fundamentals to applications. *Coord. Chem. Rev.* **2019**, *387*, 235-248.
- [15] Zhou, P.; Shi, R.; Yao, J.-f.; Sheng, C.-f.; Li, H. Supramolecular self-assembly of nucleotide-metal coordination complexes: From simple molecules to nanomaterials. *Coord. Chem. Rev.* **2015**, *292*, 107-143.
- [16] Xu, L.; Zhang, Z.; Fang, X.; Liu, Y.; Liu, B.; Liu, J. Robust hydrogels from lanthanide nucleotide coordination with evolving nanostructures for a highly stable protein encapsulation. *ACS Appl. Mater. Interfaces* **2018**, *10*, 14321-14330.
- [17] Zhang, Z.; Morishita, K.; Lin, W. T. D.; Huang, P.-J. J.; Liu, J. Nucleotide coordination with 14 lanthanides studied by isothermal titration calorimetry. *Chin. Chem. Lett.* **2018**, *29*, 151-156.
- [18] Navarro, J. A. R.; Lippert, B. Molecular architecture with metal ions, nucleobases and other heterocycles. *Coord. Chem. Rev.* **1999**, *185-186*, 653-667.
- [19] Miyake, Y.; Togashi, H.; Tashiro, M.; Yamaguchi, H.; Oda, S.; Kudo, M.; Tanaka, Y.; Kondo, Y.; Sawa, R.; Fujimoto, T.; Machinami, T.; Ono, A. MercuryII-mediated formation of thymine-Hg^{II}-thymine base pairs in DNA duplexes. *J. Am. Chem. Soc.* **2006**, *128*, 2172-2173.
- [20] Tanaka, Y.; Oda, S.; Yamaguchi, H.; Kondo, Y.; Kojima, C.; Ono, A. 15N-15N J-coupling across Hg^{II}: direct observation of Hg^{II}-mediated T-T base pairs in a DNA duplex. *J. Am. Chem. Soc.* **2007**, *129*, 244-245.
- [21] Ono, A.; Cao, S.; Togashi, H.; Tashiro, M.; Fujimoto, T.; Machinami, T.; Oda, S.; Miyake, Y.; Okamoto, I.; Tanaka, Y. Specific interactions between silver(I) ions and cytosine-cytosine pairs in DNA duplexes. *Chem. Commun.* **2008**, 4825-4827.
- [22] Torigoe, H.; Miyakawa, Y.; Nagasawa, N.; Kozasa, T.; Ono, A. Thermodynamic analyses of the specific interaction between two C:C mismatch base pairs and silver (I) cations. *Nucleic Acids Symp.* **2006**, *50*, 225-226.
- [23] Bastidas, A. C.; Deal, M. S.; Steichen, J. M.; Guo, Y.; Wu, J.; Taylor, S. S. Phosphoryl transfer by protein kinase A is captured in a crystal lattice. *J. Am. Chem. Soc.* **2013**, *135*, 4788-4798.

- [24] Liu, J.; Morikawa, M.-a.; Kimizuka, N. Conversion of molecular information by luminescent nanointerface self-assembled from amphiphilic Tb(III) complexes. *J. Am. Chem. Soc.* **2011**, *133*, 17370-17374.
- [25] Jastrzb, R.; Nowak, M.; Skrobańska, M.; Tolińska, A.; Zabiszak, M.; Gabryel, M.; Marciniak, L.; Kaczmarek, M. T. DNA as a target for lanthanide(III) complexes influence. *Coord. Chem. Rev.* **2019**, *382*, 145-159.
- [26] Pu, F.; Ren, J.; Qu, X. Nucleobases, nucleosides, and nucleotides: versatile biomolecules for generating functional nanomaterials. *Chem. Soc. Rev.* **2018**, *47*, 1285-1306.
- [27] Liu, Y.; Tang, Z. Nanoscale biocoordination polymers: Novel materials from an old topic. *Chem. Eur. J.* **2012**, *18*, 1030-1037.
- [28] Freisinger, E.; Sigel, R. K. O. From nucleotides to ribozymes—A comparison of their metal ion binding properties. *Coord. Chem. Rev.* **2007**, *251*, 1834-1851.
- [29] Peters, G. M.; Davis, J. T. Supramolecular gels made from nucleobase, nucleoside and nucleotide analogs. *Chem. Soc. Rev.* **2016**, *45*, 3188-3206.
- [30] Berti, L.; Burley, G. A. Nucleic acid and nucleotide-mediated synthesis of inorganic nanoparticles. *Nat. Nanotechnol.* **2008**, *3*, 81-87.
- [31] de Meester, P.; Goodgame, D. M. L.; Jones, T. J.; Skapski, A. C. X-ray evidence for metal–N-7 bonding in a hydrated manganese derivative of guanosine 5'-monophosphate. *Biochem. J.* **1974**, *139*, 791-792.
- [32] Clark, G. R.; Orbell, J. D. Transition-metal–nucleotide complexes. X-Ray crystal and molecular structure of the complex between nickel(II) and inosine 5'-monophosphate [Ni(imp)(H₂O)₅·2H₂O]. *J. Chem. Soc., Chem. Commun.* **1974**, 10.1039/C39740000139, 139-140.
- [33] Eichhorn, G. L.; Butzow, J. J.; Shin, Y. A. Some effects of metal ions on DNA structure and genetic information transfer. *J. Biosciences* **1985**, *8*, 527-535.
- [34] Theophanides, T.; Tajmir-Riahi, H. Flexibility of DNA and RNA upon binding to different metal cations. An investigation of the B to A to Z conformational transition by Fourier transform infrared spectroscopy. *J. Biomol. Struct. Dyn.* **1985**, *2*, 995-1004.
- [35] Andrushchenko, V.; Van de Sande, J.; Wieser, H.; Kornilova, S.; Blagoi, Y. P. Complexes of (dG-dC) 20 with Mn²⁺ ions: a study by vibrational circular dichroism and infrared absorption spectroscopy. *J. Biomol. Struct. Dyn.* **1999**, *17*, 545-560.
- [36] Duguid, J.; Bloomfield, V. A.; Benevides, J.; Thomas, G. J. Raman spectroscopy of DNA-metal complexes. I. Interactions and conformational effects of the divalent cations: Mg, Ca, Sr, Ba, Mn, Co, Ni, Cu, Pd, and Cd. *Biophys. J.* **1993**, *65*, 1916-1928.
- [37] Duguid, J. G.; Bloomfield, V. A.; Benevides, J. M.; Thomas Jr, G. J. Raman spectroscopy of DNA-metal complexes. II. The thermal denaturation of DNA in the presence of Sr²⁺, Ba²⁺, Mg²⁺, Ca²⁺, Mn²⁺, Co²⁺, Ni²⁺, and Cd²⁺. *Biophys. J.* **1995**, *69*, 2623.
- [38] Cooney, M.; Czernuszewicz, G.; Postel, E. H.; Flint, S. J.; Hogan, M. E. Site-specific oligonucleotide binding represses transcription of the human c-myc gene in vitro. *Science* **1988**, *241*, 456-459.
- [39] Bloomfield, V. A. Condensation of DNA by multivalent cations: considerations on mechanism. *Biopolymers* **1991**, *31*, 1471-1481.
- [40] Bloomfield, V. A. DNA condensation by multivalent cations. *Biopolymers* **1997**, *44*, 269-282.
- [41] Andrushchenko, V.; Tsankov, D.; Wieser, H. Vibrational circular dichroism spectroscopy and the effects of metal ions on DNA structure. *J. Mol. Struct.* **2003**, *661*, 541-560.
- [42] Liu, J.; Li, H. W.; Wang, W. X.; Wu, Y. Thermally prepared ultrabright adenosine monophosphate capped gold nanoclusters and the intrinsic mechanism. *J. Mater. Chem. B* **2017**, *5*, 3550-3556.
- [43] Zhang, L.; Wang, W.-X.; Li, A.; Liu, J.; Li, H.-W.; Wu, Y. Influence of pressure on the structure and luminescence properties of AMP-protected gold nanoparticles as revealed by fluorescence spectra and 2D correlation analysis. *J. Mol. Struct.* **2020**, *1214*, 128173.
- [44] You, Q.; Chen, Y. Ultrabright, highly heat-stable gold nanoclusters through functional ligands and hydrothermally-induced luminescence enhancement. *J. Mater. Chem. C* **2018**, *6*, 9703-9712.
- [45] Wang, Y.; Chen, T.; Zhuang, Q.; Ni, Y. One-pot aqueous synthesis of nucleoside-templated fluorescent copper nanoclusters and their application for discrimination of nucleosides. *ACS Appl. Mater. Interfaces* **2017**, *9*, 32135-32141.
- [46] Gao, Y.; Wang, G.; Gu, H.; Zhang, J.; Li, W.; Fu, Y. Cooperatively controlling the enzyme mimicking Pt nanomaterials with nucleotides and solvents. *Colloid Surf. A-Physicochem. Eng. Asp.* **2021**, *613*, 126070.
- [47] Lopez, A.; Liu, J. Light-Activated Metal-coordinated Supramolecular complexes with charge-directed self-assembly. *J. Phys. Chem. C* **2013**, *117*, 3653-3661.
- [48] Auffan, M.; Rose, J.; Bottero, J.-Y.; Lowry, G. V.; Jolivet, J.-P.; Wiesner, M. R. Towards a definition of inorganic nanoparticles from an environmental, health and safety perspective. *Nat. Nanotechnol.* **2009**, *4*, 634-641.
- [49] Pu, F.; Huang, Y.; Yang, Z.; Qiu, H.; Ren, J. Nucleotide-based assemblies for green synthesis of silver nanoparticles with controlled localized surface plasmon resonances and their applications. *ACS Appl. Mater. Interfaces* **2018**, *10*, 9929-9937.
- [50] Liu, J.; Yuan, X.-X.; Li, H.-W.; Wu, Y. Hydrothermal synthesis of novel photosensitive gold and silver bimetallic nanoclusters protected by adenosine monophosphate (AMP). *J. Mater. Chem. C* **2017**, *5*, 9979-9985.
- [51] Yu, X.; Liu, J.; Li, H. W.; Wu, Y. A two-stage assembly with PEI induced emission enhancement of Au-AgNCs@AMP and the intrinsic mechanism. *Nanoscale* **2018**, *10*, 14563-14569.

- [52] Tang, Q.; Plank, T. N.; Zhu, T.; Yu, H.; Ge, Z.; Li, Q.; Li, L.; Davis, J. T.; Pei, H. Self-assembly of metallo-nucleoside hydrogels for injectable materials that promote wound closure. *ACS Appl. Mater. Interfaces* **2019**, *11*, 19743-19750.
- [53] Sharma, B.; Mandani, S.; Thakur, N.; Sarma, T. K. Cd(II)-nucleobase supramolecular metallo-hydrogels for in situ growth of color tunable CdS quantum dots. *Soft Matter* **2018**, *14*, 5715-5720.
- [54] Sharma, B.; Mahata, A.; Mandani, S.; Thakur, N.; Pathak, B.; Sarma, T. K. Zn(II)-nucleobase metal-organic nanofibers and nanoflowers: synthesis and photocatalytic application. *New J. Chem.* **2018**, *42*, 17983-17990.
- [55] Hu, Y.; Shen, P.; Zeng, N.; Wang, L.; Yan, D.; Cui, L.; Yang, K.; Zhai, C. Hybrid hydrogel electrolyte based on metal-organic supermolecular self-assembly and polymer chemical cross-linking for rechargeable aqueous Zn-MnO₂ batteries. *ACS Appl. Mater. Interfaces* **2020**, *12*, 42285-42293.
- [56] Bairi, P.; Chakraborty, P.; Mondal, S.; Roy, B.; Nandi, A. K. A thixotropic supramolecular hydrogel of adenine and riboflavin-5'-phosphate sodium salt showing enhanced fluorescence properties. *Soft Matter* **2014**, *10*, 5114-5120.
- [57] Sukul, P. K.; Malik, S. Supramolecular hydrogels of adenine: morphological, structural and rheological investigations. *Soft Matter* **2011**, *7*, 4234.
- [58] Iwaura, R.; Yoshida, K.; Masuda, M.; Yase, K.; Shimizu, T. Spontaneous fiber formation and hydrogelation of nucleotide bolaamphiphiles. *Chem. Mat.* **2002**, *14*, 3047-3053.
- [59] Chen, J.; Liu, X.; Suo, Z.; Gao, C.; Xing, F.; Feng, L.; Zhao, C.; Hu, L.; Ren, J.; Qu, X. Right-/left-handed helical G-quartet nanostructures with full-color and energy transfer circularly polarized luminescence. *Chem. Commun.* **2020**, *56*, 7706-7709.
- [60] Nie, F.; Ga, L.; Ai, J. One-pot synthesis of nucleoside-templated fluorescent silver nanoparticles and gold nanoparticles. *ACS Omega* **2019**, *4*, 7643-7649.
- [61] Pu, F.; Qu, S.; Qiu, H.; Zhang, L. Regulation of light-harvesting antenna based on silver ion-enhanced emission of dye-doped coordination polymer nanoparticles. *J. Colloid Interface Sci.* **2020**, *578*, 254-261.
- [62] Thakur, N.; Sharma, B.; Bishnoi, S.; Mishra, S. K.; Nayak, D.; Kumar, A.; Sarma, T. K. Multifunctional inosine monophosphate coordinated metal-organic hydrogel: multistimuli responsiveness, self-healing properties, and separation of water from organic solvents. *ACS Sustain. Chem. Eng.* **2018**, *6*, 8659-8671.
- [63] Thakur, N.; Sharma, B.; Bishnoi, S.; Jain, S.; Nayak, D.; Sarma, T. K. Biocompatible Fe³⁺ and Ca²⁺ dual cross-linked G-quadruplex hydrogels as effective drug delivery system for pH-responsive sustained zero-order release of doxorubicin. *ACS Appl. Bio Mater.* **2019**, *2*, 3300-3311.
- [64] Suo, Z.; Hou, X.; Chen, J.; Liu, X.; Liu, Y.; Xing, F.; Chen, Y.; Feng, L. Highly chiroptical detection with gold-silver bimetallic nanoclusters circularly polarized luminescence based on G-quartet nanofiber self-assembly. *J. Phys. Chem. C* **2020**, *124*, 21094-21102.
- [65] Snyder, J. A.; Charnay, A. P.; Kohl, F. R.; Zhang, Y.; Kohler, B. DNA-like photophysics in self-assembled silver(I)-nucleobase nanofibers. *J. Phys. Chem. B* **2019**, *123*, 5985-5994.
- [66] Li, M.; Wang, C.; Di, Z.; Li, H.; Zhang, J.; Xue, W.; Zhao, M.; Zhang, K.; Zhao, Y.; Li, L. Engineering multifunctional DNA hybrid nanospheres through coordination-driven self-assembly. *Angew. Chem., Int. Ed.* **2019**, *58*, 1350-1354.
- [67] Liu, B.; Hu, F.; Zhang, J.; Wang, C.; Li, L. A biomimetic coordination nanoplatforM for controlled encapsulation and delivery of drug-gene combinations. *Angew. Chem., Int. Ed.* **2019**, *131*, 8896-8900.
- [68] Jia, Y.; Shen, X.; Sun, F.; Na, N.; Ouyang, J. Metal-DNA coordination based bioinspired hybrid nanospheres for in situ amplification and sensing of microRNA. *J. Mater. Chem. B* **2020**, *8*, 11074-11081.
- [69] Liu, X.; Zhang, F.; Jing, X.; Pan, M.; Liu, P.; Li, W.; Zhu, B.; Li, J.; Chen, H.; Wang, L.; Lin, J.; Liu, Y.; Zhao, D.; Yan, H.; Fan, C. Complex silica composite nanomaterials templated with DNA origami. *Nature* **2018**, *559*, 593-598.
- [70] Liu, X.; Jing, X.; Liu, P.; Pan, M.; Liu, Z.; Dai, X.; Lin, J.; Li, Q.; Wang, F.; Yang, S.; Wang, L.; Fan, C. DNA framework-encoded mineralization of calcium phosphate. *Chem* **2020**, *6*, 472-485.
- [71] Yu, X.; Hu, L.; He, H.; Zhang, F.; Wang, M.; Wei, W.; Xia, Z. Y-shaped DNA-Mediated hybrid nanoflowers as efficient gene carriers for fluorescence imaging of tumor-related mRNA in living cells. *Anal. Chim. Acta* **2019**, *1057*, 114-122.
- [72] Khalifehzadeh, R.; Arami, H. The CpG molecular structure controls the mineralization of calcium phosphate nanoparticles and their immunostimulation efficacy as vaccine adjuvants. *Nanoscale* **2020**, *12*, 9603-9615.
- [73] Li, Z.; Sun, G.; Snow, C. D.; Xu, Y.; Wang, Y.; Xiu, D.; Zhang, Y.; Zhu, Z.; Belfiore, L. A.; Tang, J. Near infrared emitting and biocompatible Yb³⁺-DNA complexes with dual responses to Cu²⁺ and Fe³⁺. *Opt. Mater.* **2020**, *108*, 110157.
- [74] Wang, S.; Chen, Y.; Wang, S.; Li, P.; Mirkin, C. A.; Farha, O. K. DNA-functionalized metal-organic framework nanoparticles for intracellular delivery of proteins. *J. Am. Chem. Soc.* **2019**, *141*, 2215-2219.
- [75] Wang, S.; McGuirk, C. M.; Ross, M. B.; Wang, S.; Chen, P.; Xing, H.; Liu, Y.; Mirkin, C. A. General and direct method for preparing oligonucleotide-functionalized metal-organic framework nanoparticles. *J. Am. Chem. Soc.* **2017**, *139*, 9827-9830.
- [76] Wang, Z.; Fu, Y.; Kang, Z.; Liu, X.; Chen, N.; Wang, Q.; Tu, Y.; Wang,

- L.; Song, S.; Ling, D.; Song, H.; Kong, X.; Fan, C. Organelle-specific triggered release of immunostimulatory oligonucleotides from intrinsically coordinated DNA-metal-organic frameworks with soluble exoskeleton. *J. Am. Chem. Soc.* **2017**, *139*, 15784-15791.
- [77] Yu, K.; Wei, T.; Li, Z.; Li, J.; Wang, Z.; Dai, Z. Construction of molecular sensing and logic systems based on site-occupying effect-modulated MOF-DNA interaction. *J. Am. Chem. Soc.* **2020**, *142*, 21267-21271.
- [78] Qiu, W.; Gao, F.; Yano, N.; Kataoka, Y.; Handa, M.; Yang, W.; Tanaka, H.; Wang, Q. Specific coordination between Zr-MOF and phosphate-terminated DNA coupled with strand displacement for the construction of reusable and ultrasensitive aptasensor. *Anal. Chem.* **2020**, *92*, 11332-11340.
- [79] Zhang, P.; Ouyang, Y.; Willner, I. Multiplexed and amplified chemiluminescence resonance energy transfer (CRET) detection of genes and microRNAs using dye-loaded hemin/G-quadruplex-modified UiO-66 metal-organic framework nanoparticles. *Chem. Sci.* **2021**, 10.1039/d0sc06744j.
- [80] Meng, H. M.; Shi, X.; Chen, J.; Gao, Y.; Qu, L.; Zhang, K.; Zhang, X. B.; Li, Z. DNA amplifier-functionalized metal-organic frameworks for multiplexed detection and imaging of intracellular mRNA. *ACS Sens.* **2020**, *5*, 103-109.
- [81] Meng, H. M.; Hu, X. X.; Kong, G. Z.; Yang, C.; Fu, T.; Li, Z. H.; Zhang, X. B. Aptamer-functionalized nanoscale metal-organic frameworks for targeted photodynamic therapy. *Theranostics* **2018**, *8*, 4332-4344.
- [82] Liu, Y.; Hou, W.; Xia, L.; Cui, C.; Wan, S.; Jiang, Y.; Yang, Y.; Wu, Q.; Qiu, L.; Tan, W. ZrMOF nanoparticles as quenchers to conjugate DNA aptamers for target-induced bioimaging and photodynamic therapy. *Chem. Sci.* **2018**, *9*, 7505-7509.
- [83] Xu, L.; Zhang, P.; Liu, Y.; Fang, X.; Zhang, Z.; Liu, Y.; Peng, L.; Liu, J. Continuously tunable nucleotide/lanthanide coordination nanoparticles for DNA adsorption and sensing. *ACS Omega* **2018**, *3*, 9043-9051.
- [84] Chen, C.; Yuan, Q.; Ni, P.; Jiang, Y.; Zhao, Z.; Lu, Y. Fluorescence assay for alkaline phosphatase based on ATP hydrolysis-triggered dissociation of cerium coordination polymer nanoparticles. *Analyst* **2018**, *143*, 3821-3828.
- [85] Zhang, C. X.; Tanner, J. A.; Li, H. W.; Wu, Y. A novel fluorescence probe of plasmodium vivax lactate dehydrogenase based on adenosine monophosphate protected bimetallic nanoclusters. *Talanta* **2020**, *213*, 120850.
- [86] Wu, S.; Tan, H.; Wang, C.; Wang, J.; Sheng, S. A colorimetric immunoassay based on coordination polymer composite for the detection of carcinoembryonic antigen. *ACS Appl. Mater. Interfaces* **2019**, *11*, 43031-43038.
- [87] Ungor, D.; Csapo, E.; Kismarton, B.; Juhasz, A.; Dekany, I. Nucleotide-directed syntheses of gold nanohybrid systems with structure-dependent optical features: Selective fluorescence sensing of Fe³⁺ ions. *Colloid Surf. B-Biointerfaces* **2017**, *155*, 135-141.
- [88] Zhan, L.; Yang, T.; Zhen, S. J.; Huang, C. Z. Cytosine triphosphate-capped silver nanoparticles as a platform for visual and colorimetric determination of mercury(II) and chromium(III). *Microchim. Acta* **2017**, *184*, 3171-3178.
- [89] Zhang, C. X.; Gao, Y. C.; Wang, C.; Yu, X.; Li, H. W.; Wu, Y. Aggregation-induced emission enhancement of adenosine monophosphate-capped bimetallic nanoclusters by aluminum(III) ions, and its application to the fluorometric determination of cysteine. *Microchim. Acta* **2019**, *187*, 41.
- [90] Zhang, Y.; Yang, M.; Shao, Z.; Xu, H.; Chen, Y.; Yang, Y.; Xu, W.; Liao, X. A paper-based fluorescent test for determination and visualization of cysteine and glutathione by using gold-silver nanoclusters. *Microchem. J.* **2020**, *158*, 105327.
- [91] Weng, Y.; Zhu, Q.; Huang, Z. Z.; Tan, H. Time-resolved fluorescence detection of superoxide anions based on an enzyme-integrated lanthanide coordination polymer composite. *ACS Appl. Mater. Interfaces* **2020**, *12*, 30882-30889.
- [92] Liang, H.; Liu, B.; Yuan, Q.; Liu, J. Magnetic iron oxide nanoparticle seeded growth of nucleotide coordinated polymers. *ACS Appl. Mater. Interfaces* **2016**, *8*, 15615-15622.
- [93] Memon, A. H.; Ding, R.; Yuan, Q.; Liang, H.; Wei, Y. Coordination of GMP ligand with Cu to enhance the multiple enzymes stability and substrate specificity by co-immobilization process. *Biochem. Eng. J.* **2018**, *136*, 102-108.
- [94] Liang, H.; Sun, S.; Zhou, Y.; Liu, Y. In-situ self-assembly of Zinc/adenine hybrid nanomaterials for enzyme immobilization. *Catalysts* **2017**, *7*, 327.
- [95] Gao, J.; Wang, C.; Tan, H. Lanthanide/nucleotide coordination polymers: an excellent host platform for encapsulating enzymes and fluorescent nanoparticles to enhance ratiometric sensing. *J. Mater. Chem. B* **2017**, *5*, 7692-7700.
- [96] Liang, H.; Jiang, S.; Yuan, Q.; Li, G.; Wang, F.; Zhang, Z.; Liu, J. Co-immobilization of multiple enzymes by metal coordinated nucleotide hydrogel nanofibers: improved stability and an enzyme cascade for glucose detection. *Nanoscale* **2016**, *8*, 6071-6078.
- [97] Zhao, C. X.; Zhang, X. P.; Shu, Y.; Wang, J. H. Europium-pyridinedicarboxylate-adenine light-up fluorescence nanoprobe for selective detection of phosphate in biological fluids. *ACS Appl. Mater. Interfaces* **2020**, *12*, 22593-22600.
- [98] Gao, R.; Wang, J.; Wang, H.; Dong, W.; Zhu, J. Fluorescent nucleotide-lanthanide nanoparticles for highly selective determination of picric acid. *Microchim. Acta* **2021**, *188*, 18.
- [99] Ma, S.; Hu, Y.; Zhang, Q.; Guo, Z.; Wang, S.; Shen, Q.; Liu, C.; Liu, Z.

- Adenine/Au complex-dependent versatile electrochemical platform for ultrasensitive DNA-related enzyme activity assay. *Sens. Actuator B-Chem.* **2018**, *273*, 760-770.
- [10] Liu, Y.; Peng, L.-L.; Huang, W.-X.; Zhou, H.-Z.; Xu, L. Luminescent nucleotide/Tb³⁺ coordination polymer for Fe(II) detection in human serum. *Anal. Methods* **2020**, *12*, 1122-1130.
- [101] Liu, L.; Jiang, H.; Wang, X. Bivalent metal ions tethered fluorescent gold nanoparticles as a reusable peroxidase mimic nanozyme. *J. Anal. Test.* **2019**, *3*, 269-276.
- [102] Chen, L.; Xu, H.; Wang, L.; Li, Y.; Tian, X. Portable ratiometric probe based on the use of europium(III) coordination polymers doped with carbon dots for visual fluorometric determination of oxytetracycline. *Microchim. Acta* **2020**, *187*, 125.
- [103] Zhang, G.; Quin, M. B.; Schmidt-Dannert, C. Self-assembling protein scaffold system for easy in vitro coimmobilization of biocatalytic cascade enzymes. *ACS Catal.* **2018**, *8*, 5611-5620.
- [104] Garcia, J.; Zhang, Y.; Taylor, H.; Cespedes, O.; Webb, M. E.; Zhou, D. Multilayer enzyme-coupled magnetic nanoparticles as efficient, reusable biocatalysts and biosensors. *Nanoscale* **2011**, *3*, 3721-3730.
- [105] Mehta, J.; Bhardwaj, N.; Bhardwaj, S. K.; Kim, K.-H.; Deep, A. Recent advances in enzyme immobilization techniques: metal-organic frameworks as novel substrates. *Coord. Chem. Rev.* **2016**, *322*, 30-40.
- [106] He, J.; Sun, S.; Lu, M.; Yuan, Q.; Liu, Y.; Liang, H. Metal-nucleobase hybrid nanoparticles for enhancing the activity and stability of metal-activated enzymes. *Chem. Commun.* **2019**, *55*, 6293-6296.
- [107] Jiang, Y.; Liu, S.; Yuan, Q.; Liang, H. Zr-based acid-stable nucleotide coordination polymers: An excellent platform for acidophilic enzymes immobilization. *J. Inorg. Biochem.* **2021**, *216*, 111338.
- [108] Wu, X.; Liu, S.; Xiong, J.; Chen, B.; Zong, M.-H.; Yang, J.-G.; Lou, W.-Y. In-situ construction of enzyme-copper nucleotide composite for efficient chemo-enzymatic cascade reaction. *Appl. Catal. A-Gen.* **2020**, *608*, 117899.
- [109] Li, C.; Jiang, S.; Zhao, X.; Liang, H. Co-immobilization of enzymes and magnetic nanoparticles by metal-nucleotide hydrogel nanofibers for improving stability and recycling. *Molecules* **2017**, *22*, 179.
- [110] Jiang, D.; Ni, D.; Rosenkrans, Z. T.; Huang, P.; Yan, X.; Cai, W. Nanozyme: new horizons for responsive biomedical applications. *Chem. Soc. Rev.* **2019**, *48*, 3683-3704.
- [111] Li, Y.; Liu, J. Nanozyme's catching up: activity, specificity, reaction conditions and reaction types. *Mater. Horizons* **2021**, *8*, 336-350.
- [112] Wu, J.; Wang, X.; Wang, Q.; Lou, Z.; Li, S.; Zhu, Y.; Qin, L.; Wei, H. Nanomaterials with enzyme-like characteristics (nanozymes): next-generation artificial enzymes (II). *Chem. Soc. Rev.* **2019**, *48*, 1004-1076.
- [113] Huang, Y.; Ren, J.; Qu, X. Nanozymes: classification, catalytic mechanisms, activity regulation, and applications. *Chem. Rev.* **2019**, *119*, 4357-4412.
- [114] Tao, X.; Wang, X.; Liu, B.; Liu, J. Conjugation of antibodies and aptamers on nanozymes for developing biosensors. *Biosens. Bioelectron.* **2020**, *168*, 112537.
- [115] Lopez, A.; Liu, J. Coordination nanoparticles formed by fluorescent 2-aminopurine and Au³⁺: stability and nanozyme activities. *J. Anal. Test.* **2019**, *3*, 219-227.
- [116] Zhang, C.-X.; Gao, Y.-C.; Li, H.-W.; Wu, Y. Gold-platinum bimetallic nanoclusters for oxidase-like catalysis. *ACS Appl. Nano Mater.* **2020**, *3*, 9318-9328.
- [117] Peng, D.; Liang, R.-P.; Qiu, J.-D.; Liu, J. Robust colorimetric detection of Cu²⁺ by excessed nucleotide coordinated nanozymes. *J. Anal. Test.* **2019**, *3*, 260-268.
- [118] Liang, H.; Lin, F.; Zhang, Z.; Liu, B.; Jiang, S.; Yuan, Q.; Liu, J. Multicopper laccase mimicking nanozymes with nucleotides as ligands. *ACS Appl. Mater. Interfaces* **2017**, *9*, 1352-1360.
- [119] Jiao, M.; Li, Z.; Li, X.; Zhang, Z.; Yuan, Q.; Vriesekoop, F.; Liang, H.; Liu, J. Solving the H₂O₂ by-product problem using a catalase-mimicking nanozyme cascade to enhance glycolic acid oxidase. *Chem. Eng. J.* **2020**, *388*, 124249.
- [120] Wang, G.; Feng, L.; Li, W.; Zhang, J.; Fu, Y. In-situ generation of nanozymes by natural nucleotides: a biocatalytic label for quantitative determination of hydrogen peroxide and glucose. *Microchim. Acta* **2019**, *186*, 514.
- [121] Zou, T.; Han, Y.; Li, X.; Li, W.; Zhang, J.; Fu, Y. Unexpected catalytic activity of Pd(II)-coordinated nucleotides in hydrogenation reduction. *Colloid Surf. A-Physicochem. Eng. Asp.* **2019**, *560*, 344-351.
- [122] Huang, Z.; Liu, B.; Liu, J. A high local DNA concentration for nucleating a DNA/Fe coordination shell on gold nanoparticles. *Chem. Commun.* **2020**, *56*, 4208-4211.
- [123] Liu, Y.; Liu, J. Growing a nucleotide/lanthanide coordination polymer shell on liposomes. *Langmuir* **2019**, *35*, 11217-11224.
- [124] Yang, Y. C.; Wang, Y. T.; Tseng, W. L. Amplified peroxidase-like activity in iron oxide nanoparticles using adenosine monophosphate: application to urinary protein sensing. *ACS Appl. Mater. Interfaces* **2017**, *9*, 10069-10077.
- [125] You, J. G.; Wang, Y. T.; Tseng, W. L. Adenosine-related compounds as an enhancer for peroxidase-mimicking activity of nanomaterials: application to sensing of heparin level in human Pplasma and total sulfate glycosaminoglycan content in synthetic cerebrospinal fluid. *ACS Appl. Mater. Interfaces* **2018**, *10*, 37846-37854.
- [126] Chandra, V.; Park, J.; Chun, Y.; Lee, J. W.; Hwang, I.-C.; Kim, K. S. Water-dispersible magnetite-reduced graphene oxide composites for arsenic removal. *ACS Nano* **2010**, *4*, 3979-3986.
- [127] Yue, Q.; Li, J.; Luo, W.; Zhang, Y.; Elzatahry, A. A.; Wang, X.; Wang, C.; Li, W.; Cheng, X.; Alghamdi, A.; Abdullah, A. M.; Deng, Y.; Zhao, D. An interface coassembly in biphase: toward core-shell magnetic

- mesoporous silica microspheres with tunable pore size. *J. Am. Chem. Soc.* **2015**, *137*, 13282-13289.
- [128] Deng, Y.; Qi, D.; Deng, C.; Zhang, X.; Zhao, D. Superparamagnetic high-magnetization microspheres with an Fe₃O₄@SiO₂ core and perpendicularly aligned mesoporous SiO₂ shell for removal of microcystins. *J. Am. Chem. Soc.* **2008**, *130*, 28-29.
- [129] Xu, Z.; Hou, Y.; Sun, S. Magnetic core/shell Fe₃O₄/Au and Fe₃O₄/Au/Ag nanoparticles with tunable plasmonic properties. *J. Am. Chem. Soc.* **2007**, *129*, 8698-8699.
- [130] Jones, M. R.; Seeman, N. C.; Mirkin, C. A. Programmable materials and the nature of the DNA bond. *Science* **2015**, *347*, 1260901.
- [131] Song, Z.-L.; Zhao, X.-H.; Liu, W.-N.; Ding, D.; Bian, X.; Liang, H.; Zhang, X.-B.; Chen, Z.; Tan, W. Magnetic graphitic nanocapsules for programmed DNA fishing and detection. *Small* **2013**, *9*, 951-957.
- [132] Zhang, S.; Lin, F.; Yuan, Q.; Liu, J.; Li, Y.; Liang, H. Robust magnetic laccase-mimicking nanozyme for oxidizing o-phenylenediamine and removing phenolic pollutants. *J. Environ. Sci.* **2020**, *88*, 103-111.
- [133] Zhang, X.; Deng, J.; Xue, Y.; Shi, G.; Zhou, T. Stimulus response of Au-NPs@GMP-Tb core-shell nanoparticles: toward colorimetric and fluorescent dual-mode sensing of alkaline phosphatase activity in algal blooms of a freshwater lake. *Environ. Sci. Technol.* **2016**, *50*, 847-855.
- [134] Nishiyabu, R.; Aime, C.; Gondo, R.; Kaneko, K.; Kimizuka, N. Selective inclusion of anionic quantum dots in coordination network shells of nucleotides and lanthanide ions. *Chem. Commun.* **2010**, *46*, 4333-4335.
- [135] Yang, Y.; Zhu, W.; Feng, L.; Chao, Y.; Yi, X.; Dong, Z.; Yang, K.; Tan, W.; Liu, Z.; Chen, M. G-quadruplex-based nanoscale coordination polymers to modulate tumor hypoxia and achieve nuclear-targeted drug delivery for enhanced photodynamic therapy. *Nano Lett.* **2018**, *18*, 6867-6875.
- [136] Jiang, K.; Chen, Y.; Zhao, D.; Cheng, J.; Mo, F.; Ji, B.; Gao, C.; Zhang, C.; Song, J. A facile and efficient approach for hypertrophic scar therapy via DNA-based transdermal drug delivery. *Nanoscale* **2020**, *12*, 18682-18691.
- [137] Bhattacharyya, T.; Chaudhuri, R.; Das, K. S.; Mondal, R.; Mandal, S.; Dash, J. Cytidine-Derived Hydrogels with Tunable Antibacterial Activities. *ACS Appl. Bio Mater.* **2019**, *2*, 3171-3177.
- [138] Zhang, T.; Nong, J.; Alzahrani, N.; Wang, Z.; Oh, S. W.; Meier, T.; Yang, D. G.; Ke, Y.; Zhong, Y.; Fu, J. Self-assembly of DNA-minocycline complexes by metal ions with controlled drug release. *ACS Appl. Mater. Interfaces* **2019**, *11*, 29512-29521

